The cellular Notch1 Protein Promotes KSHV reactivation in an Rta-dependent manner.

Jennifer DeCotiis-Mauro[a,b]+, Sun M. Han[a,b]+, Helena Mello[a,b], Corey Goyeneche[a,b], Giuseppina Marchesini-Tovar[a,b], Lianhua Jin[a,b], Vivian Bellofatto[a,b], and David M. Lukac[a,b]#

[a] Dept of Microbiology, Biochemistry, and Molecular Genetics, Rutgers Biomedical and Health Sciences, New Jersey Medical School, Rutgers University, Newark, NJ

[b]School of Graduate Studies, Rutgers Biomedical and Health Sciences, Health Science Campus at Newark, Rutgers University, Newark, NJ

Running Head: Notch1 contributes to KSHV reactivation

#Corresponding author: E-mail: Lukacdm@njms.rutgers.edu

+ authors contributed equally to this work

Abstract: 239 words

Abstract

The cellular Notch signal transduction pathway is intimately associated with infections by Kaposi's sarcoma-associated herpesvirus (KSHV) and other gamma-herpesviruses. RBP-Jk, the cellular DNA binding component of the canonical Notch pathway, is the key Notch downstream effector protein in virus-infected and uninfected animal cells. Reactivation of KSHV from latency requires the viral lytic switch protein, Rta, to form complexes with RBP-Jk on numerous sites within the viral DNA. Constitutive Notch activity is essential for KSHV pathophysiology in models of Kaposi's sarcoma (KS) and Primary Effusion Lymphoma (PEL), and we demonstrate that Notch1 is also constitutively active in infected Vero cells. Although the KSHV genome contains >100 RBP-Jk DNA motifs, we show that none of the four isoforms of activated Notch can productively reactivate the virus from latency in a highly quantitative trans-complementing reporter virus system. Nevertheless, Notch contributed positively to reactivation because broad inhibition of Notch1-4 with gamma secretase inhibitor (GSI) or expression of dominant negative mastermind-like1 (dnMAML1) coactivators severely reduced production of infectious KSHV from Vero cells. Reduction of KSHV production is associated with gene specific reduction of viral transcription in both Vero and PEL cells. Specific inhibition of Notch1 by siRNA partially reduces production of infectious KSHV, and NICD1 forms promoter-specific complexes with viral DNA during reactivation. We conclude that constitutive Notch activity is required for robust production of infectious KSHV, and our results implicate activated Notch1 as a pro-viral member of a MAML1/RBP-Jk/DNA complex during viral reactivation.

51 **Importance**

52 Kaposi's sarcoma-associated herpesvirus (KSHV) manipulates the host cell oncogenic Notch
53 signaling pathway for viral reactivation from latency and cell pathogenesis. KSHV reactivation requires
54 that the viral protein Rta functionally interacts with RBP-Jk, the DNA binding component of the Notch
55 pathway, and with promoter DNA to drive transcription of productive cycle genes. We show that the
56 Notch pathway is constitutively active during KSHV reactivation and is essential for robust production
57 of infectious virus progeny. Inhibiting Notch during reactivation reduces expression of specific viral
58 genes yet does not affect growth of the host cells. Although Notch cannot reactivate KSHV alone, the
59 requisite expression of Rta reveals a previously unappreciated role for Notch in reactivation. We
60 propose that activated Notch cooperates with Rta in a promoter-specific manner that is partially
61 programmed by Rta's ability to redistribute RBP-Jk DNA binding to the virus during reactivation.
62

63 **Introduction**

64 Human gammaherpesviral infections and pathogenesis are dependent on interactions of the virus
65 with the cellular Notch signal transduction pathway (1). In uninfected cells, the canonical model of
66 Notch signaling involves activation of the Notch protein by proteolytic release of the Notch Intracellular
67 Domain (NICD)1 from the membrane-associated Notch1 receptor (2, 3). NICD1 then translocates to the
68 cell nucleus, binds to DNA-bound Recombination signal binding protein (RBP)-Jk and activates
69 transcription by displacing a transcriptional co-repressor complex from RBP-Jk and assembling a
70 transcriptional co-activator complex.

71 Reactivation of the gammaherpesvirus Kaposi's sarcoma-associated herpesvirus (KSHV)
72 requires the KSHV Replication and transcriptional activator (Rta) to assemble a complex with RBP-Jk
73 and DNA to activate transcription of essential viral genes (4-27). Reflecting the central roles of Rta and
74 RBP-Jk in reactivation, the KSHV genome contains greater than 100 consensus RBP-Jk DNA motifs,
75 and Rta and RBP-Jk co-occupy many viral promoters during reactivation in B cells (28). However,
76 although both Rta and NICD1 target RBP-Jk, we and others have shown that only Rta is sufficient to
77 productively reactivate KSHV in B cell models of latency (6, 29). Indeed, our recent work showed that
78 ectopic expression of Rta in infected Vero cells induced profound production of infectious virus assayed
79 by a robust and sensitive trans-complementing reporter virus-cell system (30). In parallel experiments,
80 this highly sensitive assay revealed that ectopic expression of NICD1 failed to produce detectable virus
81 (30). Thus, this highly sensitive reactivation system confirmed conclusions from human B cell studies
82 and is ideal to compare transcriptional mechanisms of Rta and Notch.

83 Despite ectopic NICD1's insufficiency to reactivate KSHV alone, the literature suggests that
84 Notch signaling contributes to regulation of KSHV infection. Notch can activate viral productive cycle
85 genes without inducing complete reactivation in B and endothelial cell models of latency (29, 31). In
86 infected primary effusion lymphoma (PEL) cells, conditionally-expressed NICD1 activated a subset of

87 viral genes that were different than those activated by Rta (29). Nevertheless, a broader review of the
88 literature shows that our understanding of Notch's role in KSHV reactivation remains debatable. One
89 study concluded that ectopic NICD1 is capable of inducing complete reactivation (32) by directly
90 activating Rta's promoter and a second study indicated that Notch inhibits reactivation in neighboring
91 cells by indirectly repressing Rta expression (33). The interpretation of experiments intended to analyze
92 the role of Notch signaling in KSHV reactivation are complicated by two observations: first, Notch
93 signaling is constitutively-active in all KSHV-infected cells, and second, one or more of the activated
94 Notch proteins (i.e. NICD1-4) is required for growth and survival of KSHV-infected cells (31, 34-40).
95 Indeed, Notch isoforms 1, 2, and 4, Notch activating ligands, and numerous Notch target genes are
96 overexpressed and active in KS lesional tissue, PEL cells, and in KSHV-infected endothelial cells.
97 Notch signaling is also reciprocally impacted by KSHV infection in myriad and complex ways.
98 The expression of Notch ligands and receptors are increased by specific latent and lytic viral proteins,
99 including Rta, in infected lymphatic endothelial cells (31, 35, 37-39). Notch signaling is reprogramed
100 when the viral immediate early protein Rta stimulates RBP-Jk DNA binding and by proteolytic
101 processing of Notch effector proteins (6, 9, 28, 41). Rta-dependent stimulation of RBP-Jk binding to the
102 KSHV Mta promoter converts it to a Notch-responsive gene (6). Moreover, our ChIP/Seq studies
103 demonstrated that RBP-Jk binding to the viral genome is dramatically redistributed during reactivation,
104 but Rta and RBP-Jk do not co-occupy every newly identified RBP-Jk site (28). Taken together, these
105 data suggest that Notch plays an essential and complementary role with Rta in KSHV reactivation.
106 While it is clear that Rta is the only viral protein that is necessary and sufficient to reactivate the
107 complete KSHV lytic cycle, a complete understanding of Rta's reactivation function must consider the
108 intracellular environment that is replete with potent, constitutive Notch activity.
109 In the present study, we use the KSHV-infected Vero cell model and multiple complementary
110 methodologies to demonstrate that Notch signaling is key to viral reactivation. Specifically, we

111 demonstrate that exposing infected cells to the Notch small-molecule-inhibitor DAPT, or to Notch-
112 inhibiting dominant negative Mastermind-like (dmMAML)-1, severely reduces production of infectious
113 KSHV. Reactivation reduction occurs after either chemical induction of virus or forced expression of
114 Rta. Inhibition of KSHV virion production is accompanied by reduction of selected viral transcripts and
115 proteins. Importantly, reactivation stymied by DAPT treatment is not the result of cell growth reduction
116 by the drug. While we show that none of the four Notch isoforms are sufficient to reactivate the virus,
117 transfection of specific siRNAs implicates Notch 1 as one of the isoforms that contribute to Rta-induced
118 reactivation. We observe formation of specific Notch1/DNA complexes on the viral genome during
119 reactivation. Finally, we also observe a block in reactivation, which is measured here by a decrease in
120 viral DNA production, by inhibiting Notch in naturally KSHV-infected PEL cells. Taken together, our
121 study illustrates that although Rta is necessary and sufficient for KSHV reactivation, viral reactivation
122 relies on continued endogenous Notch signaling, likely by working with Rta cooperatively during the
123 early steps of reactivation.
124
125
126

127 **Materials and Methods**

128

129 **Plasmids:** All plasmids were grown in DH5α *E. coli* and purified using the cesium chloride maxi-prep
130 method (42). All prepared plasmids were confirmed via restriction enzyme digestion and/or sequencing.
131 pcDNA3-FLg50 expresses full length Rta protein from a genomic allele of KSHV ORF50 (43).
132 pCAGGS:dnMAML1-GFP and pEGFP-N1-dnMAML1 express dominant negative mutants of MAML1
133 fused to GFP and were gifts of Dr. Signe V. Horn Pederson (44). pEGFP-N1-H2b (referred to as H2b-
134 GFP) expresses GFP-fused histone H2b and was a gift of Dr. Geoff Wahl (Addgene plasmid #11680)
135 (45). pcDNA3.1-HisLacZ (13) expresses β-galactosidase reporter protein under control of the HCMV
136 enhancer. The reporter plasmids 4xCSL-luciferase (Addgene plasmid #41726) and 4xCBS-luciferase
137 encode firefly luciferase under the control of four RBP-Jk binding sites are were gifts of Dr. Raphael
138 Kopan and Dr. Rhett Kovall, respectively (46, 47). p3xFLAG-NICD 1-4 express Notch intracellular
139 domains (NICD) 1-4 from the p3xFLAG-CMV-7 expression vector and were gifts of Dr. Raphael
140 Kopan (48). pcDNA3.1-ORF50ΔSTADV5 expresses transcriptionally inert, dominant negative KSHV
141 Rta (nts 1-1590) fused to the V5 epitope tag (13). pCMV-NICDΔPEST, NICD1-P12, NICD1-L1594P
142 express NICD1 alleles containing different activating mutations found in human T cell acute
143 lymphoblastic leukemia cells provided by Dr. Jon C. Aster (49). pcDNA3 (Invitrogen) was used as an
144 empty vector control ("Vec") and DNA filler for all experiments.

145

146 **Cell Culture:** 293 MSR-tet OFF and Vero rKSHV.294 cells (gifts of Dr. Jeff Vieira) were maintained
147 as previously described (30, 50). BC3 cells (a gift of Dr. Ethel Cesarman) and BCBL-1 cells were
148 maintained in RPMI medium supplemented with 12% or 10% Fetal Bovine Serum (FBS) respectively,
149 1% glutamine, 50uM β-mercaptoethanol, and 1% penicillin/streptomycin.
150 Viral reactivation was induced chemically by treatment of cells with 1 mM Valproic acid (VPA;

151 Sigma, P4543; prepared in dH_2O and filtered through 0.22uM surfactant-free cellulose acetate (SFCA)).
152 Notch activity was inhibited chemically by treatment of cells with (2*S*)-*N*-[(3,5-
153 Difluorophenyl)acetyl]-L-alanyl-2-phenyl]glycine 1,1-dimethylethyl ester (DAPT; Selleckchem,
154 S2215); concentrations are given in the figure legends. The solvent vehicle for DAPT was dimethyl
155 sulfoxide (DMSO), which was used as the control, vehicle ("Vh") treatment in all experiments.
156
157
158 **Transfections:** Vero rKSHV.294 cells were plated at a concentration of $2x10^5$ cells per well of 6-well
159 plates and incubated at 37°C overnight. The following day, 2.5 ug of total plasmid DNA and 5 uL of
160 vortexed TransIT-LT1 reagent were added to 250 uL incomplete DMEM and incubated at RT for 30m.
161 The mixture was added to the Vero rKSHV.294 cells dropwise, and cells were incubated for 48 or 72h at
162 37°C, for protein harvest or SeAP assay respectively. Specific plasmids used in transfections are
163 indicated in respective figure legends.
164 For siRNAs, Vero rKSHV.294 cells were plated at a concentration of $2x10^5$ cells per well of six-
165 well plates and incubated overnight at 37° C. The following day, 30 pmol of either control siRNA-A
166 (Santa Cruz, sc-37007), Notch 1 siRNA (h) A (Santa Cruz, sc36095A), or Notch 1 siRNA (h2) (Santa
167 Cruz, sc-44226A) were diluted in 150 uL of incomplete DMEM and mixed with 9 uL of Lipofectamine
168 RNAiMAX reagent previously diluted in incomplete DMEM per manufacturers' suggestions. The
169 mixtures were incubated for 5m at RT, then added to cells.
170
171 **Secreted Alkaline Phosphatase (SeAP) Assay:** Virus-containing media from Vero rKSHV.294 cells
172 were transferred to 293 MSR-tet-OFF cells previously plated at a density of $2x10^5$ cells/well in 6-well
173 plates 24h earlier. 293 MSR-tet-OFF cells were returned to the incubator for 72h (unless otherwise
174 indicated) at 37°C. SeAP-containing media were harvested, and 20 or 25 uL were assayed using either
175 the Great EscAPe SeAP kit (Takara/Clontech) or the Phospha-Light System (Applied Biosystems).

176

177 **Protein extractions and assays**: Cells were washed with 1x PBS, and lysed using RIPA buffer (150
178 mM NaCl, 1% NP40, 0.5% sodium deoxycholate, 0.1% SDS, 50 mM Tris pH 8.0) supplemented with
179 protease inhibitor cocktail (Sigma P2714) and 1 mM DTT. Dishes were scraped, contents were
180 transferred to microfuge tubes, debris was pelleted by centrifugation, and supernatants were transferred
181 to new microfuge tubes. Total protein concentrations were determined by Protein Assay (Bradford; Bio-
182 Rad).

183 For luciferase and β-galactosidase quantitation, at 48h post-transfection, cells were washed twice
184 with 1x PBS, then lysed in 125 uL 1x reporter lysis buffer (Promega) for 20min at RT. Dishes were
185 scraped, contents were transferred to microfuge tubes, debris was pelleted by centrifugation, and
186 supernatants were transferred to new microfuge tubes. Luciferase activity was measured in the BD
187 monolight 3010 luminometer (BD Biosciences) using 20 uL of each extract into which 20 uL luciferase
188 assay substrate was injected (Promega). β-galactosidase activity was measured by absorbance at 420 nm
189 in the Tecan Genios plate reader using 30 uL of each extract mixed with 30 uL of 2x Assay Buffer
190 (Promega).

191

192 **SDS-PAGE and Western Blotting:** Protein samples were mixed with 6x Laemmli buffer containing
193 freshly added β-mercaptoethanol, heated at 95°C for 5m, then loaded on gels. Proteins were transferred
194 via electroblotting to nitrocellulose (Main Manufacturing LLC) or PVDF (GVS Filter Tech 1212783;
195 PVDF membranes only were initially dipped in 100% methanol). Membranes were blocked with 5%
196 milk in 1x PBS/0.1% Tween 20 (blocking buffer) for at least 30m, then washed with 1x PBS/0.1%
197 Tween 20 and 1x PBS. Primary antibodies were diluted in blocking buffer then incubated with the blots
198 for 4h at RT or overnight at 4°C; antibodies and dilutions were as follows: anti-Notch1 (1:200, Santa
199 Cruz sc-32745, or bTAN20 Developmental Studies Hybridoma Bank, deposited by Dr. Spyros

200 Artavanis-Tsakonas), anti-Rta (1:4000, D3861 (14)), anti-FLAG (1:1000, M2 Sigma Aldrich F1804, or
201 PA1-984B Thermo scientific), anti-GAPDH (1:1000, BioLegend 919501), anti-GFP (1:200, B-2 Santa
202 Cruz sc-9996) anti-ORF59 (1H10; (14)), anti-KbZIP (51) or anti-Mta (52). The membranes were then
203 washed with 1x PBS/0.1% Tween 20 and 1x PBS and incubated for 30m with secondary antibodies
204 diluted in blocking buffer; antibodies and dilutions were as follows: Goat anti-Mouse IgG-h+1 HRP
205 conjugated (1:5000, Bethyl Labs A90-116P), Rabbit TruBlot anti-Rabbit IgG (1:1000, Rockland 18-
206 8816-33), Goat anti-Rabbit IgG-h+1 HRP conjugated (1:5000, Bethyl A120-101P). Membranes were
207 partially dried and incubated for up to 2m in Pierce ECL Western Blotting Substrate (Thermo Scientific,
208 32016). Signals were detected by exposure to autoradiography film (Denville, E3012) for up to 24h, or
209 digitally captured using myECL imager (Thermo Scientific) or Chemidoc (BioRad).
210
211 **Quantitative Reverse Transcription-real-time Polymerase Chain Reaction (RT-qPCR)** Total RNA
212 was extracted from Vero rKSHV.294 cells using the RNeasy kit (Qiagen) as per manufacturer's
213 suggestions. DNA contamination was removed using the TURBO DNA-free kit (Invitrogen) as per
214 manufacturer's suggestions. Transcripts were quantitated by qRT-PCR using the iTaq Universal SYBR
215 Green One-Step Kit (Bio-Rad) following manufacturer's suggestions. 5 to 100 ng. of input RNA was
216 amplified using KSHV-specific unique coding sequence primers (53) or β-actin primers (54) in a
217 CFX96/C1000 instrument (Bio-Rad). Reaction conditions were 10 mins 50ºC for RT, 1 min 95ºC, then
218 40 cycles of 10 sec 95ºC/10 sec 60ºC. Amplification specificity was confirmed for all primer pairs by
219 melt-curve analysis and parallel control reactions that lacked template RNA or reverse transcriptase.
220
221 **vDNA quantitation:** BC3 cells were treated with indicated chemicals for 65h and total DNA was
222 purified from cell lysates using the FlexiGene DNA kit (Qiagen). Intracellular viral DNA was measured
223 by real-time quantitative (q) PCR of the viral genome; GAPDH was the internal control. qPCR reactions

224 were performed using SYBR Green PCR Master Mix (Thermo Scientific). Input DNA (100 ng) was
225 amplified by incubating at 50°C for 10m and 95°C for 10m, then cycled 39 times with melting at 95°C
226 for 15 sec and annealing at 60°C for 1m. Fold DNA was calculated using the ΔCt method and all values
227 were normalized to that of VPA + vehicle, which was set to 100%.
228
229 **Immunofluorescence**: Cells were harvested in 15 mL conical tubes, washed twice with 1x Phosphate
230 Buffered Saline (PBS), and resuspended at a density of $1.25x10^6$ cells/mL in 1x PBS. 15-20 mm circles
231 were drawn on glass microscope slides with a Super PAP pen (ThermoFisher 008899), then coated by a
232 10m incubation with 4 uL poly-L-lysine. Polylysine was removed, 200 uL of cells/circle were adhered
233 for 30m, then fixed in pre-chilled methanol/acetone (50/50 v/v) at -20°C for 5 to 10min. Slides were air
234 dried for 10min at RT and cells were blocked with 3% BSA/1% glycine in 1x PBS. The following
235 primary antibodies were diluted in 1:1000 in blocking buffer and incubated for 1h with the cells: anti-
236 Rta (D3861; (14)), anti-K8.1 (Santa Cruz Bio sc-65446, 1:1000), or anti-ORF59 (1H10; (14)). Cells
237 were washed with 1x PBS/0.4% Tween20 and 1x PBS, then the following secondary antibodies were
238 diluted 1:500 in blocking buffer and incubated for 1h with the cells: anti-rabbit DyLight 448 (Thermo
239 Scientific, 35552), anti-rabbit DyLight 550 (Thermo Scientific, 84541), or anti-mouse DyLight 550
240 (Thermo Scientific, 84540). Cells were re-washed, and coverslips were mounted to slides using Vecta-
241 shield with DAPI (Vector Labs).
242
243 **Cell Growth Quantitation:** Vero rKSHV.294 cells were plated at a density of 6.7×10^3 cells/well of a
244 96-well dish. 24 h later, cells were treated with 1 uL vehicle alone (control) or containing DAPT (final
245 concentration of 1 or 5 uM), in triplicate. Three mock wells were also prepared with media only for
246 each time point. At the post-treatment times indicated, cell media was replaced with 200 uL growth
247 assay media (180 uL DME + 20 uL Alamar Blue (BioRad BUF012A), and incubation was continued for

248 4 hr at 37°C. Alamar Blue fluorescence was measured by excitation at 544 nm/emission at 590 nm in a
249 SpectraMax M2 plate reader (Molecular Devices). Mock values were averaged and subtracted from
250 each experimental value to yield corrected values. All corrected values were then normalized to 0h
251 values that had been set to the relative value of 1 for each treatment.

252 **Chromatin Immunoprecipitation (ChIP)/Polymerase Chain Reaction (PCR):** Modified from (55,
253 56). Vero rKSHV.294 cells were plated at (1.5x10^6 cells per 100mm plate). 24h later, cells were
254 transfected in triplicate with 12.5 ug total of pcDNA3 or pcDNA3-FLg50 using TransIT LT1 (Mirus)
255 per manufacturer's protocol. 24h after transfection, chromatin was cross-linked by replacing growth
256 medium with 8 mL of serum-free medium containing 1.42% methanol-free formaldehyde (Peirce) and
257 incubating for 8m at room temperature. Formaldehyde was quenched with 125 mM glycine for 5m at
258 room temperature, then washed twice with 10 mL ice cold 1x PBS. Cells were scraped into fresh 10 mL
259 of ice cold 1x PBS, transferred to 15 mL conical tubes, and combined with an additional 2 mL of 1x
260 PBS that was used to rinse residual cells from each plate. Cells were pelleted by centrifugation at
261 2000g, 5m, at 4° C. Pellets from single plates were lysed by resuspension in 1 mL of ChIP buffer (150
262 mM NaCl, 50 mM Tris-HCl (pH 7.5), 5 mM EDTA, 0.5% v/v NP-40, 1.0% v/v Triton X-100, and
263 supplemented with protease inhibitor cocktail (Sigma P2714) by repeated slow-pipetting after transfer to
264 1.5 mL Bioruptor Micro tubes (Diagenode) on ice. Incubation on ice was continued for 10m, and
265 nuclear pellets were recovered by centrifugation at 12,000g for 1m at 4° C. Nuclear pellets were
266 resuspended in 300 uL sonication buffer (ChIP buffer plus 1.0% v/v Sodium dodecyl-sulfate), and
267 chromatin sonicated in the Bioruptor Pico (Diagenode) to average size of 250 bp (typically 15 cycles of
268 30s on/30s off, vortexing every 5 cycles). Nuclear lysates were as cleared by centrifugation at 12,000g,
269 10m, 4° C, and aliquoted in 2 million cell equivalents per subsequent ChIP. Some chromatin was set
270 aside for analysis of input quality and quantity.

271 ChIPs were performed by adding anti-NICD1 antibody (Cell Signaling 3608) or equal amounts
272 of non-specific rabbit IgG (Sigma PP64) to individual chromatin aliquots: 0.55 or 1 ug of each antibody
273 were added to 1 million or 2 million cell equivalents, respectively. ChIPs were incubated 16-24h at 4° C
274 with nutation. Chromatin was cleared by centrifugation at 12000g for 10 mins at 4° C and mixed with
275 magnetic Protein A/G beads (Cytiva 17152104010150) that had been prewashed with ChIP buffer and
276 blocked with ChIP buffer/1% v/v Bovine Serum Albumin. ChIP'd chromatin was recovered by
277 incubating with beads for 45m at 4° C with nutation. Beads were washed 6 times with 1 mL each of
278 ChIP buffer on a magnetic tube rack (Invitrogen). After removing the final wash, DNA was recovered
279 by resuspending the magnetic beads in 100 uL 10% w/v Chelex 100/d$H_2$0 suspension (Bio-Rad) and
280 boiling the mixture for 10m. After cooling, proteins were removed by adding 20 ug of Proteinase K,
281 vortexing, and incubating on a thermal mixer at 55° C for 30m at 1000 rpm. Proteinase K was
282 inactivated by boiling samples for 10m, then centrifuged for 1m at 12000g, 4° C. 80 uLs of supernatant
283 was transferred to new tubes. Fresh 120 uLs of dH_2O was added to the Chelex resin, vortexed for 10s,
284 and centrifugation repeated. 120 uL of that supernatant was removed and mixed with first 80 uL aliquot.

285 Purified DNA was analyzed using real-time qPCR with SYBR green (Applied Biosystems
286 4472918); primer sequences are available upon request. Fold enrichment of NICD1 on vDNA was
287 calculated using the ΔΔCt method, comparing the Ct for anti-NICD1 to IgG first for each sample, then
288 EV to Rta-transfected samples second. Final folds were determined by scaling to input chromatin and
289 amount of NICD1 expression in each condition. Data shown represent results of four independent
290 transfections performed in duplicate or triplicate, and ChIP'd twice per transfection. Two ChIPs from
291 one transfection used alternate control non-specific IgG (Cell Signaling 2729S) or anti-GFP (Cell
292 Signaling 2956) to confirm results.

293

294 **Results**

295 **Notch1 is constitutively active in KSHV-infected Vero cells**

296 To understand the complex interactions of Notch signaling with KSHV infection, we have
297 employed an infected Vero cell model. These cells have emerged as a robust system for understanding
298 host and viral regulation of productive KSHV reactivation. Infected Vero cells provide a number of
299 improvements over other reactivation models, including their ease of transfection. Gantt and colleagues
300 (50) developed a Vero cell line that produces a recombinant KSHV reporter virus upon reactivation that
301 is quantifiable by infecting a trans-complementing 293 cell line. Using this system, we previously
302 demonstrated that ectopic, activated Notch1 (NICD1) was insufficient to produce infectious virus,
303 confirming work from studies of PEL cells (6, 29, 30).

304 Many cellular models of KSHV infection demonstrate constitutive activation of NICD1 (31, 34,
305 36-38) which is required to maintain cell growth and survival (36-38). Based on the dramatic
306 association of Notch activity with KSHV infection in those cells, we sought to determine the status of
307 Notch1 in infected Vero cells. We prepared total protein extracts from infected Vero cells that were
308 grown for 24h. Western blotting with anti-Notch1-specific antisera demonstrated a protein band doublet
309 that migrated with an apparent molecular weight (MW) of 100-120 kDa (Fig. 1). The doublet matched
310 the pattern and migration of the bands observed from control, uninfected Vero cells transfected with an
311 NICD1 expression vector (Fig. 1 "Con"). Therefore, we conclude that Notch1 is constitutively active in
312 latent, KSHV-infected Vero cells. Others have shown that expression of one or several productive cycle
313 KSHV proteins could induce expression of Notch pathway components in 293 cells (39). However, we
314 found that treating the infected Vero cells with VPA to reactivate the virus did not increase the
315 constitutively high amount of NICD1 in the cells (not shown).

316

317
318

319 **Inhibiting Notch activation reduces KSHV reactivation**

320 To determine whether endogenous, constitutive Notch activity contributed to KSHV reactivation,
321 we measured the effect of DAPT treatment on mature infectious virus production from Vero
322 rKSHV.294 cells. Cells were pre-treated with DAPT or the vehicle control ("Vh"; DMSO) for 24h, then
323 transfected with Rta expression vector to induce viral reactivation or empty vector (Vec) control. When
324 Notch is active, which is the case in the Vh only cultures, ectopic Rta reactivates virus to approximately
325 700-fold greater than Vec, as we previously published (Fig. 2A) (30). In cells where Notch is inhibited,
326 which is the case in the DAPT-treated cells, and viral reactivation is attempted by Rta addition,
327 reactivation is stymied. These data suggest that constitutive Notch activity is necessary for optimal viral
328 growth (Fig. 2A).

329 Since reactivation is scored by transferring the supernatants from the infected Vero cells to 293
330 MSR tet-OFF cells, we performed a key control experiment to assess the potential effect of DAPT on
331 the function of the 293 reporter cells. We treated virus-containing supernatant media from the
332 experimental Vero rKSHV.294 cells with DAPT prior to incubating the supernatants with the 293 cells.
333 There was no decrease in virus detection in the 293 cells, confirming that DAPT does not inhibit *de*
334 *novo* infection by KSHV nor expression of the SEAP reporter protein (not shown).

335 To confirm that NICD activity was reduced by DAPT treatment in the infected Vero cells, we co-
336 transfected the Vero rKSHV.294 cells with two reporter plasmids. One contained four RBP-Jk motifs
337 arrayed in tandem upstream of a luciferase reporter gene, and the other contained the HCMV enhancer
338 sequence lacking RBP-Jk motifs for normalization. As expected, treatment of the cells with 5 uM
339 DAPT for 6 or 24h reduced Notch activity relative to vehicle-treated cells (Fig. 2B).

340 To determine if viral gene expression was similarly debilitated by inhibiting Notch activation
341 during reactivation, we measured levels of viral transcripts in the infected Vero cells. We observed a
342 gene specific reduction in viral RNAs (Figs 2C and D) in cells where Notch is inhibited (+DAPT) and

343 viral reactivation is induced by ectopic Rta. The expression of K2, ORF74, ORF8, ORF6, ORF34, and
344 K8.1 transcripts were significantly reduced by inhibiting Notch transactivation with DAPT (Figs 2C and
345 D). ORF6 and ORF55 transcripts followed the same trend of sensitivity to Notch inhibition with DAPT,
346 but did not reach statistical significance (Fig 2D). K14 transcript was activated by Rta expression but not
347 reduced by Notch inhibition, and ORF72 transcription was neither induced by Rta expression or
348 repressed by DAPT pre-treatment (Fig 2C). We conclude that activated Notch supports production of
349 infectious KSHV by transactivating specific, essential viral genes in cooperation with Rta.
350

351 **Inhibiting Notch activation does not reduce growth of KSHV-infected Vero cells**

352 Notch inhibition by DAPT can inhibit growth and induce apoptosis in KSHV-infected cells (31,
353 34-40). To determine the effect of DAPT on growth of the infected Vero rKSHV.294 cells, we
354 measured cell viability by alamarBlue sensitivity. Over a 72h period of growth, cells treated with 1 uM
355 or 5 uM DAPT maintained normal cell viability (Fig. 2E). The Fig. 2 data therefore support the
356 conclusion that Notch inhibition by DAPT treatment specifically reduces viral reactivation without
357 affecting Vero cell growth or viability.
358

359 **Inhibiting the Notch transactivation complex reduces KSHV reactivation**

360 Inhibiting the gamma-secretase complex with DAPT can block the formation of several signaling
361 substrates in addition to Notch (57). Therefore, we worked to specifically block Notch activity directly
362 at its site of transcriptional transactivation by testing the effects of ectopically expressing dominant
363 negative (dn) mutants of the Mastermind-like1 (MAML1) protein. Cognate MAML1 stabilizes the
364 NICD1/RBP-Jk/DNA complex to facilitate NICD1-dependent transactivation in the nucleus (2, 3, 58,
365 59). Transfection of Vero rKSHV.294 cells with two different dnMAML1 expression vectors reduced

366 Rta-mediated reactivation by 40% or 90%, respectively (Fig. 3A). As a control, we observed that
367 dnMAML1 proteins were strongly expressed (Fig 3B).
368 To determine if viral gene expression was similarly debilitated by inhibiting the Notch
369 transactivation complex during reactivation, we measured protein levels in the infected Vero cells. We
370 observed a gene specific reduction in viral proteins (Figs 3C and D) in cells expressing dnMAML1
371 relative to empty vector-transfected cells. The expression of Mta and KbZIP proteins were significantly
372 reduced by inhibiting Notch transactivation with dnMAML1. Taken together with Fig 2, we conclude
373 that activated Notch supports production of infectious KSHV by transactivating specific, essential viral
374 genes in cooperation with Rta.
375
376 **Notch1 is necessary for optimal viral reactivation**
377
378 The data in Figs. 2 and 3 show that inhibiting Notch post-translationally at two different
379 biochemical steps of its activation dramatically reduced KSHV reactivation and support a pro-viral role
380 for Notch signaling in viral reactivation in Vero cells. However, these experiments do not specify which
381 of the four Notch receptors, Notch1,2,3 or 4, are required for efficient reactivation, as all four proteins
382 are inhibited by DAPT and ectopic dnMAML1 (2, 58, 60-64).
383 Since Notch1 is constitutively active in Vero cells, we asked whether specific knock-down of
384 Notch1 would affect viral reactivation. We transfected two different siRNAs to knock-down
385 endogenous Notch1 in Vero-rKSHV.294 cells, and then induced viral reactivation by transfection of Rta
386 expression vector (Fig. 4A) or treatment with the HDAC inhibitor valproic acid (VPA; eg. the most
387 potent chemical inducer of viral reactivation in Vero cells (65)) (Fig. 4B). The Notch1-specific siRNAs
388 reduced viral reactivation in all cases relative to control, scrambled siRNA ("Scr"), up to a maximum of
389 ~80% inhibition ("N1-B" in Fig. 4A). Knock-down of endogenous Notch1 was confirmed via Western

390 blot (Fig 4C). These data verify that constitutively active Notch1 plays a pro-viral role in KSHV
391 reactivation in Vero cells.

392 **Activated Notch1 binds to viral promoter DNA during KSHV reactivation.**
393
394 Our observations that inhibiting Notch during KSHV reactivation reduced viral gene
395 transcription without affecting cell growth (Figs. 2 and 3) suggested that our observed proviral function
396 of Notch1 (Fig 4) is to transactivate specific viral genes to support KSHV reactivation. Activated
397 Notch1 (NICD1) transactivates specific cellular genes by assembling NICD1/MAML1/RBP-Jk1/DNA
398 complexes on promoters or enhancers (2, 3, 58, 59). We and others have demonstrated that RBP-Jk1
399 binds to many sites on KSHV DNA (4-27), and we have mapped eighty-two RBP-Jk1 binding sites to
400 the viral genome during reactivation (55). We selected six RBP-Jk1 binding sites found within 1 kb
401 upstream of transcription start sites for KSHV genes, ie. in their presumptive promoters, and asked
402 whether we could also detect NICD1 occupancy there using chromatin immunoprecipitation. When we
403 induced reactivation in rKSHV.294 cells by transfecting Rta expression vector, qPCR showed that
404 NICD1 antibody co-precipitated significantly more promoter DNA than in EV-transfected cells on the
405 K2, ORF34, ORF6, ORF8, and the bidirectional ORF50AS/K8 promoters (Fig. 5). Transcription of four
406 of these genes was significantly impaired when Notch activity was inhibited (Figs 2C and D). We
407 conclude that NICD1 forms complexes with RBP-Jk and DNA to transactivate specific viral genes to
408 support KSHV reactivation.
409

410 **Notch is pro-viral in PEL cells**
411
412 Notch1 is constitutively active in PEL cells (36-38). To determine whether Notch1 also supports
413 reactivation in these cells, we reactivated virus with VPA in the presence of 16, 32, or 40 uM of DAPT
414 and quantitated vDNA accumulation and protein expression. DAPT reduced intracellular vDNA
415 accumulation up to a maximum of ~80% relative to VPA plus vehicle control ("Vh") (Fig 6A). DAPT

416 also reduced the percentage of K8.1-positive cells (Fig. 6B); as K8.1 is a true-late gene, this result was
417 consistent with the effect of DAPT on vDNA accumulation. Interestingly, we did not observe an effect
418 of DAPT treatment on the percentage of ORF59-positive cells, perhaps because our assay was not
419 designed to detect modest effects on the ORF59 amounts or signal intensity (Fig 6B).
420 In an SLK cell model of KSHV infection, Notch was shown to inhibit reactivation and reduce
421 expression of productive cycle genes, including Rta (33). In contrast, we did not observe a statistically
422 significant effect of DAPT treatment on Rta expression in any of the experiments we performed in
423 Vero and PEL cells (not shown).
424
425 **Ectopic, activated Notch isoforms 1 to 4 are insufficient to reactivate KSHV from latency**
426 In our experiments using the infected Vero cell system, as well as experiments in PEL cells, we
427 demonstrated that ectopic NICD1 is incapable of productively reactivating KSHV, despite widespread
428 RBP-Jk binding to the latent viral genome (6, 9, 30). Although other Notch isoforms are commonly
429 constitutively-expressed in KSHV-infected cells (31, 34, 36-38) it is possible that their endogenous
430 levels are insufficient to drive viral reactivation. To test whether ectopic Notch isoforms 2, 3, and 4
431 could reactivate KSHV, we transfected vectors that express NICD 2, 3, and 4 into Vero rKSHV.294
432 cells. As expected, ectopic Rta, the positive control, gave a 500-fold increase in KSHV reactivation as
433 measured by SeAP activity (Fig. 7A). However, little to no virus was detectable from cells transfected
434 with any of the NICD expression vectors (NICD1, 1.1-fold; NICD2, 9.4-fold; NICD3, 2.9-fold; NICD4,
435 4.8-fold), similar to effects in cells transfected with the Rta transcriptionally deficient mutant
436 ORF50ΔSTAD (1.7-fold; Fig. 7A). All four isoforms were thus insufficient to reactivate KSHV from
437 Vero cells, despite their robust expression levels (Fig 7B).
438
439 **Ectopic NICD1 and 2 are transactivation competent in KSHV-infected Vero cells**

440 It is possible that the activated Notch proteins are unable to reactivate KSHV because they are not
441 transcriptionally active in Vero rKSHV.294 cells. To assess their activities, we co-transfected Vero
442 rKSHV.294 cells with a reporter vector containing four tandem RBP-Jκ sites, and each of the four NICD
443 expression vectors at the same amounts as in Fig 7. We observed significant transactivation of this
444 promoter by both NICD1 and 2, but not NICD3 or 4 (Fig 8). Taken together with Fig. 7, these data
445 confirm that NICD1 and 2 are incapable of reactivating KSHV despite being transcriptionally active.
446 However, the inability of NICD3 or 4 to activate transcription in these cells provides a potential
447 explanation for their inability to reactivate KSHV from latency.
448

449 **NICD mutants of varying activity are insufficient to reactivate KSHV from latency**

450 To determine whether varying the potency of ectopic, activated NICD1 could reactivate KSHV,
451 we tested a series of constitutively-active Notch alleles with varying intrinsic signaling strengths that
452 had been cloned from clinical T cell acute lymphoblastic leukemia (T-ALL) lymphomas (49, 66). Each
453 of these Notch alleles contain distinct mutations that render the protein more stable (NICDΔPEST) or
454 promote constitutive cleavage and activation (P12 and L1594P). NICDΔPEST was classified as a very
455 weak allele as it was unable to influence hematopoiesis or induce T-ALL but was found to cooperate
456 with other T-ALL initiators, including c-myc. NICD-L1594P was classified as having weak signal
457 strength due to its ability to affect hematopoiesis, but not induce T-ALL, while NICD-P12 was
458 considered a strong mutant due to its ability to induce T-ALL. We transfected vectors expressing each
459 of these alleles into the Vero rKSHV.294 cells and found that none could reactivate the virus, similar to
460 the result with cognate NICD1 ("WT"; Fig 9). These data further verify that NICD1 is insufficient to
461 reactivate KSHV from latency, regardless of its inherent potency.
462

463 **NICD1 cooperates with VPA in reactivation**

464 Our data showed that endogenous Notch1 is constitutively active in infected Vero cells and
465 supports optimal viral reactivation that is induced by VPA treatment or by ectopic Rta expression.
466 However, increasing activated Notch1 amounts alone, via ectopic NICD1 expression, was insufficient to
467 productively reactivate KSHV. To determine whether ectopic NICD1 could cooperate with VPA
468 treatment, we transfected the Vero rKSHV.294 cells with the NICD1 expression vector alone or with 1
469 mM VPA treatment. In positive control samples treated with VPA alone, we observe approximately
470 350-fold reactivation (Fig 10). As expected, ectopic expression of NICD1 alone was insufficient to
471 produce virus (Fig 10). However, expression of ectopic NICD1 in VPA-treated cells enhanced
472 reactivation to about 700-fold (Fig 10), supporting a cooperative role for NICD1 and VPA.
473
474

475 **Discussion**

476 In this work, we demonstrate that ectopic expression of activated Notch1 is insufficient to
477 productively reactivate KSHV from latency (Fig 7). NICD1's reactivation insufficiency confirms our
478 earlier results from ectopic expression of NICD1 in PEL and Vero cells (6, 30), and agrees with similar
479 results in which NICD1 was conditionally-induced ectopically in a stably-transfected PEL cell line (29).
480 To ensure that this negative result is not due to an inadequate dose of ectopic NICD1, we show that three
481 additional Notch1 alleles that encode constitutively active NICD1 proteins with varied intrinsic
482 transcriptional potency also fail to reactivate KSHV from latency (Fig 9). Our work is the first to test all
483 four of the NICD isoforms in this capacity, and conclusively establishes that ectopic NICD2 is also not
484 capable of reactivating the virus. While ectopic expression of NICD isoforms 3 and 4 also did not result
485 in production of infectious virus, we are unable to conclude that NICD3 and 4 are similarly insufficient
486 to reactivate KSHV since we could not determine that they are transcriptionally active in our
487 experiments (Fig 8). However, since the Notch isoforms have been shown to have different promoter
488 transactivation specificities (48, 67-69), it is possible that NICD3 and 4 are, in fact, active in Vero cells,

489 but are simply incapable of activating the 4x tandem RBP-Jk motif (4x CBS) reporter plasmid. NICD1
490 and 2 have been suggested to be functionally interchangeable in other biologic systems (70-72).
491 Despite Notch's inability to reactivate latent KSHV alone, we show that constitutive Notch1
492 activity is required for robust reactivation of the virus. All three of our strategies that inhibited
493 endogenous Notch activity in the Vero cells decreased Rta or VPA-induced reactivation over a range of
494 60-90% (Figs 2 to 5). Two of the strategies, DAPT treatment and dnMAML1 expression, are well-
495 established strategies to broadly inhibit all four Notch isoforms (2, 58, 60-64). DAPT blocks gamma-
496 secretase activation of endogenous Notch and dnMAML1 interferes with the formation of Notch
497 transactivation complexes (46, 73-75). However, neither strategy is strictly Notch-specific, because each
498 also interferes with other cellular processes that require gamma-secretase activity or cognate MAML1
499 (57, 59). To inhibit Notch1 specifically, we knocked-down its expression using two different transfected
500 siRNAs (Fig. 4). Inhibiting Notch with dnMAML1 reduced reactivation more dramatically than did
501 siRNA knock-down, suggesting that endogenous Notch 2, 3, and 4 may also have pro-viral functions
502 (compare Figs 3 and 4). Our Notch inhibition studies focused primarily on quantitating production of
503 infectious virus from latently infected Vero cells, but we also observed that inhibiting Notch in PEL
504 cells reduced synthesis of intracellular viral DNA (Fig 6). Those data suggest that Notch activity in both
505 cell lines have similar effects on viral infection. We note a single contradictory study that concluded that
506 ectopic NICD1 reactivated KSHV (32).
507 It is well-established that Notch signaling is critical for cell and animal models of KSHV
508 pathogenesis; however, our data are the first to demonstrate that Notch activation is necessary for robust
509 production of infectious virus. Productive cycle gene expression is also seen in the context of sustained
510 Notch activation that is required for the endothelial to mesenchymal transition of KSHV-infected cells
511 (31, 35, 39, 40). Growth and survival of KSHV-infected cells also depend on Notch activity:
512 proliferation rates of KSHV-infected B cells were proportional to Notch expression levels, and Notch

513 inhibition reduced cellular cyclin D1 expression and arrested cells in G1 (37). Moreover, pharmacologic
514 Notch inhibition induced apoptosis of infected SLK, B, and primary KS tumor cells (31, 34, 35, 37-40)
515 and induced necrosis of PEL xenografts in NOD/SCID mice (36). Although Notch1 expression is
516 insufficient to productively reactivate KSHV, ectopic Notch1 could induce expression of a subset of
517 productive cycle viral genes in PEL cells (29). Importantly, the infected Vero cell model used in our
518 work is ideal for uncoupling the effect of Notch on cell growth from its effect on viral reactivation; in
519 our work, we used DAPT concentrations that significantly reduced production of infectious virus
520 without affecting host cell doubling time or survival (Fig 2E). This pro-viral role of Notch follows the
521 paradigm established in foundational tumor virus studies in which cellular oncogenic pathways
522 manipulated by SV40 or Adenovirus also support productive viral infections (76).
523 Our data raised two intriguing questions: how does activated Notch contribute to reactivation and
524 why is it not sufficient to reactivate KSHV alone? Since complete Notch ablation is inconsistent with
525 survival of KSHV-infected cells, one apparent contribution of activated Notch is to maintain survival of
526 cells in which KSHV is reactivating (31, 34, 36-40). To this end, we note that none of our strategies to
527 reduce Notch activity were 100% effective in debilitating virus production. However, our observation
528 that DAPT treatment and partial NICD1 knock-down can debilitate reactivation without reducing cell
529 growth suggests a function of Notch that is complementary to Rta and independent of cell survival.
530
531 Our data also show that NICD1 is transactivation competent in latently-infected Vero cells (Fig
532 7), as has also been demonstrated in latently-infected PEL cells (29). Thus, all of the components
533 sufficient to form the Notch1 transactivation complex must be expressed and functional in KSHV-
534 infected cells (reviewed in (2, 3, 77)). Therefore, we believe that Notch's insufficiency to reactivate
535 KSHV derives from a limit to gene-specific transactivation that is relieved when Rta is expressed.
536 Importantly, one critical gene which ectopic NICD1 fails to activate in Vero and PEL cells is Rta (data

537 not shown; (29)). Therefore, when endogenous Rta is induced by VPA, or Rta is expressed ectopically,
538 endogenous NICD1 then likely transactivates specific viral genes during reactivation. Indeed, Notch
539 forms complexes with vDNA in the presumptive promoters of five viral genes (Fig 5), and Notch
540 inhibition is associated with reduction in expression of four of the genes and others not tested (Figs 2
541 and 3). Our observation that broad Notch inhibitors have greater anti-viral potency than specific Notch1
542 inhibition (compare Figs 2A and 3A to Fig 4A) suggests that at least one additional Notch isoform also
543 supports optimal KSHV reactivation.

544 We interpret our data as revealing that Notch activity had no influence on productive reactivation
545 unless Rta was expressed. Activated Notch has no intrinsic DNA binding ability, but instead relies upon
546 the cellular DNA binding protein RBP-Jk to specify NICD1's target genes (2, 3, 78) . One function of
547 Rta which can profoundly influence the ability of NICD1 to transactivate specific genes is Rta's ability
548 to stimulate RBP-Jk DNA binding (6, 9, 28). Our lab modeled this mechanism by showing that NICD1
549 can transactivate the Mta promoter only if a truncated form of Rta, lacking its transactivation domain,
550 stimulates RBP-Jk binding to the promoter (6). Studying the intact virus, we showed that KSHV
551 reactivation is associated with dramatic re-localization of RBP-Jk to unique sites on the virus genome
552 (28). The extent of dynamic RBP-Jk binding to the virus can be contrasted with that observed on the cell
553 genome. In uninfected cells, RBP-Jk binding sites on the cellular genome are classified as static or
554 dynamic, and NICD1 can stimulate RBP-Jk DNA binding to cellular genomes (79-82). However, on the
555 KSHV genome, the proportion of dynamic RBP-Jk sites in our studies vastly exceed the proportion of
556 dynamic sites reported on cellular genomes (28, 79, 80, 83-86). In fact, the number of reactivation-
557 specific RBP-Jk sites on the virus, and the number of RBP-Jk DNA motifs on the virus, exceed the
558 number of KSHV ORFs (28). Moreover, Rta is not found bound to the virus at every RBP-Jk site (28).
559 We hypothesize that NICD1/MAML1/RBP-Jk complexes transactivate specific essential viral promoters
560 and cooperate with Rta to support KSHV reactivation (Fig 9). During latency, in the absence of Rta

561 expression, NICD1/RBP-Jk fails to form a competent transactivation complex on at least one essential
562 viral promoter. Unlike NICD1, Rta also binds DNA independent of RBP-Jk for transactivation and
563 replication (87-90); these mechanistic differences probably also contribute to Notch's insufficiency in
564 reactivation.

565 Based on experimental data, we have published two mechanisms that describe how Rta regulates
566 RBP-Jk DNA binding: (1) Rta directly binds to RBP-Jk, and (2) Rta induces expression of additional
567 cellular proteins during reactivation which in turn bind to DNA adjacent to RBP-Jk (6, 9, 27, 28). The
568 latter mechanism is consistent with our work and others that demonstrated that *de novo* gene expression
569 downstream of Rta is required for robust reactivation (5, 27). Thus, NICD1 transactivation in KSHV-
570 infected cells is determined by the fate of the infection (latent vs. reactivating) and intracellular context,
571 as well as the DNA context of individual RBP-Jk binding sites. Similar context-dependent determinants
572 have been invoked to explain cell-specific variations in NICD1 transactivation and phenotypic
573 consequences in uninfected cells (48, 86, 91-100). The influence of cellular context on Notch function
574 includes interactions between the four Notch isoforms, including competition, cooperation, or
575 redundancy (68, 70, 71, 101-114).

576 In Notch cancer biology, cell context is a major determinant of the striking observation that
577 Notch can be either tumor suppressive or oncogenic in different malignancies (reviewed in (2, 115-
578 117)). The ideal DNA context for an NICD1-responsive RBP-Jk site is a head-to-head configuration
579 with a second RBP-Jk site spaced 15-17 nts apart (118-121); remarkably, only six pairs of RBP-Jk
580 motifs in the KSHV genome are found in that DNA context (not shown). It is likely that the mechanisms
581 underlying contextual variations in Notch signaling outcomes in uninfected cells are functionally similar
582 in KSHV infection, but uniquely regulated by KSHV proteins like Rta. Moreover, cell context may be
583 responsible for the discordance of our observations with a publication that showed that NICD1 inhibits
584 KSHV reactivation in SLK cells (33).

585 In summary, herein we demonstrate the significance of constitutive Notch1 activity in the
586 cellular context of productive KSHV reactivation. The essentiality of Rta/RBP-Jk/DNA complexes in
587 driving reactivation is well-established, but this current study demonstrates that Notch contributes to
588 reactivation by forming promoter-specific NICD1/RBP-Jk/DNA complexes, also. The KSHV genome
589 contains >100 RBP-Jk motifs of varying sequence found in varying DNA contexts that we expect to
590 respond differently to Rta and/or NICD1 to determine the success of a reactivation signal leading to
591 virus production. Moreover, our data indicate that Notch isoforms other than the well-studied Notch1
592 may help regulate viral infection. This diversity in the molecular players underlies the consequences of
593 RBP-Jk-dependent gene expression in KSHV infection and host cell pathology. Our data are consistent
594 with the idea that the Notch-dependance of viral reactivation is a complex network that, when revealed,
595 will provide important new insights into Notch-dependent signaling in mammalian cells.
596

597 **Acknowledgements**

598 We gratefully thank Drs. Jeff Vieira, Ethel Cesarman, Signe V. Horn Pederson, Geoff Wahl, Rhett
599 Kovall, Raphael Kopan, Jon C. Aster, and Spyros Artavanis-Tsakonas for cells, antibody, and plasmids.
600 The work was supported by NIH Grants AI117127 and AI150230.
601

602 **References**

603 1. Watanabe T, Sugimoto A, Hosokawa K, Fujimuro M. 2018. Signal Transduction Pathways
604 Associated with KSHV-Related Tumors. Adv Exp Med Biol 1045:321-355.
605 2. Aster JC, Pear WS, Blacklow SC. 2017. The Varied Roles of Notch in Cancer. Annu Rev Pathol
606 12:245-275.
607 3. Giaimo BD, Gagliani EK, Kovall RA, Borggrefe T. 2021. Transcription Factor RBPJ as a
608 Molecular Switch in Regulating the Notch Response, p 9-30. *In* Reichrath J, Reichrath S (ed),
609 Notch Signaling in Embryology and Cancer: Notch Signaling in Cancer doi:10.1007/978-3-030-
610 55031-8_2. Springer International Publishing, Cham.
611 4. Campbell M, Watanabe T, Nakano K, Davis RR, Lyu Y, Tepper CG, Durbin-Johnson B, Fujimuro
612 M, Izumiya Y. 2018. KSHV episomes reveal dynamic chromatin loop formation with domain-
613 specific gene regulation. Nat Commun 9:49.

614 5. Papp B, Motlagh N, Smindak RJ, Jin Jang S, Sharma A, Alonso JD, Toth Z. 2019. Genome-Wide
615 Identification of Direct RTA Targets Reveals Key Host Factors for Kaposi's Sarcoma-Associated
616 Herpesvirus Lytic Reactivation. J Virol 93.
617 6. Carroll KD, Bu W, Palmeri D, Spadavecchia S, Lynch SJ, Marras SA, Tyagi S, Lukac DM. 2006.
618 Kaposi's Sarcoma-associated herpesvirus lytic switch protein stimulates DNA binding of RBP-
619 Jk/CSL to activate the Notch pathway. J Virol 80:9697-709.
620 7. Liang Y, Chang J, Lynch S, Lukac DM, Ganem D. 2002. The lytic switch protein of KSHV
621 activates gene expression via functional interaction with RBP-Jk, the target of the Notch signaling
622 pathway. Genes Dev 16:1977-89.
623 8. Liang Y, Ganem D. 2003. Lytic but not latent infection by Kaposi's sarcoma-associated
624 herpesvirus requires host CSL protein, the mediator of Notch signaling. Proc Natl Acad Sci U S A
625 100:8490-5.
626 9. Palmeri D, Carroll KD, Gonzalez-Lopez O, Lukac DM. 2011. Kaposi's sarcoma-associated
627 herpesvirus Rta tetramers make high-affinity interactions with repetitive DNA elements in the Mta
628 promoter to stimulate DNA binding of RBP-Jk/CSL. J Virol 85:11901-15.
629 10. Hilton IB, Dittmer DP. 2012. Quantitative analysis of the bidirectional viral G-protein-coupled
630 receptor and lytic latency-associated nuclear antigen promoter of Kaposi's sarcoma-associated
631 herpesvirus. J Virol 86:9683-95.
632 11. Bu W, Carroll KD, Palmeri D, Lukac DM. 2007. The Kaposi's Sarcoma-associated
633 Herpesvirus/Human herpesvirus-8 ORF50/Rta Lytic Switch Protein Functions as a Tetramer. J
634 Virol 81:5788-5806.
635 12. Lukac D, Garibyan L, Kirshner J, Palmeri D, Ganem D. 2001. DNA binding by the Kaposi's
636 sarcoma-associated herpesvirus lytic switch protein is necessary for transcriptional activation of
637 two viral delayed early promoters. J Virol 75:6786-99.
638 13. Lukac DM, Kirshner JR, Ganem D. 1999. Transcriptional activation by the product of open
639 reading frame 50 of Kaposi's sarcoma-associated herpesvirus is required for lytic viral reactivation
640 in B cells. J Virol 73:9348-61.
641 14. Lukac DM, Renne R, Kirshner JR, Ganem D. 1998. Reactivation of Kaposi's sarcoma-associated
642 herpesvirus infection from latency by expression of the ORF 50 transactivator, a homolog of the
643 EBV R protein. Virology 252:304-312.
644 15. Wang Y, Yuan Y. 2006. Essential role of RBP-Jkappa in activation of the K8 delayed-early
645 promoter of Kaposi's sarcoma-associated herpesvirus by ORF50/RTA. Virology.
646 16. Persson LM, Wilson AC. 2010. Wide-scale use of Notch signaling factor CSL/RBP-Jkappa in
647 RTA-mediated activation of Kaposi's sarcoma-associated herpesvirus lytic genes. J Virol 84:1334-
648 47.
649 17. Scholz BA, Harth-Hertle ML, Malterer G, Haas J, Ellwart J, Schulz TF, Kempkes B. 2013.
650 Abortive lytic reactivation of KSHV in CBF1/CSL deficient human B cell lines. PLoS Pathog
651 9:e1003336.
652 18. Lan K, Kuppers DA, Verma SC, Robertson ES. 2004. Kaposi's sarcoma-associated herpesvirus-
653 encoded latency-associated nuclear antigen inhibits lytic replication by targeting Rta: a potential
654 mechanism for virus-mediated control of latency. J Virol 78:6585-94.
655 19. Liu Y, Cao Y, Liang D, Gao Y, Xia T, Robertson ES, Lan K. 2008. Kaposi's sarcoma-associated
656 herpesvirus RTA activates the processivity factor ORF59 through interaction with RBP-Jkappa
657 and a cis-acting RTA responsive element. Virology 380:264-75.
658 20. Liang Y, Ganem D. 2004. RBP-J (CSL) is essential for activation of the K14/vGPCR promoter of
659 Kaposi's sarcoma-associated herpesvirus by the lytic switch protein RTA. J Virol 78:6818-26.

660 21. Chang PJ, Boonsiri J, Wang SS, Chen LY, Miller G. 2010. Binding of RBP-Jkappa (CSL) protein
661 to the promoter of the Kaposi's sarcoma-associated herpesvirus ORF47 (gL) gene is a critical but
662 not sufficient determinant of transactivation by ORF50 protein. Virology 398:38-48.
663 22. Izumiya Y, Izumiya C, Hsia D, Ellison TJ, Luciw PA, Kung HJ. 2009. NF-kappaB serves as a
664 cellular sensor of Kaposi's sarcoma-associated herpesvirus latency and negatively regulates K-Rta
665 by antagonizing the RBP-Jkappa coactivator. J Virol 83:4435-46.
666 23. Sun R, LIn SF, Gradoville L, Yuan Y, Zhu F, Miller G. 1998. A viral gene that activates lytic cycle
667 expression of Kaposi's sarcoma-associated herpesvirus. Proc Natl Acad Sci USA 95:10866-10871.
668 24. Gradoville L, Gerlach J, Grogan E, Shedd D, Nikiforow S, Metroka C, Miller G. 2000. Kaposi's
669 sarcoma-associated herpesvirus open reading frame 50/Rta protein activates the entire lytic cycle
670 in the HH-B2 primary effusion lymphoma cell line. J Virol 74:6207-6212.
671 25. Nakamura H, Lu M, Gwack Y, Souvlis J, Zeichner SL, Jung JU. 2003. Global changes in Kaposi's
672 sarcoma-associated virus gene expression patterns following expression of a tetracycline-inducible
673 Rta transactivator. J Virol 77:4205-20.
674 26. Xu Y, AuCoin DP, Huete AR, Cei SA, Hanson LJ, Pari GS. 2005. A Kaposi's sarcoma-associated
675 herpesvirus/human herpesvirus 8 ORF50 deletion mutant is defective for reactivation of latent
676 virus and DNA replication. J Virol 79:3479-87.
677 27. Bu W, Palmeri D, Krishnan R, Marin R, Aris VM, Soteropoulous P, Lukac DM. 2008.
678 Identification of Direct Transcriptional Targets of the KSHV Rta Lytic Switch Protein by
679 conditional nuclear localization. J Virol 82:10709-10723.
680 28. Gonzalez-Lopez O DJ, Goyeneche C, Mello H, Vicente-Ortiz BA, Shin HJ, Driscoll KE, Du P,
681 Palmeri D, Lukac DM. . 2019. A herpesvirus transactivator and cellular POU proteins extensively
682 regulate DNA binding of the host Notch signaling protein RBP-Jκ to the virus genome. . J Biol
683 Chem 294:13073-13092.
684 29. Chang H, Dittmer DP, Chul SY, Hong Y, Jung JU. 2005. Role of Notch signal transduction in
685 Kaposi's sarcoma-associated herpesvirus gene expression. J Virol 79:14371-82.
686 30. DeCotiis JL, Ortiz NC, Vega BA, Lukac DM. 2017. An easily transfectable cell line that produces
687 an infectious reporter virus for routine and robust quantitation of Kaposi's sarcoma-associated
688 herpesvirus reactivation. J Virol Methods 247:99-106.
689 31. Cheng F, Pekkonen P, Laurinavicius S, Sugiyama N, Henderson S, Gunther T, Rantanen V,
690 Kaivanto E, Aavikko M, Sarek G, Hautaniemi S, Biberfeld P, Aaltonen L, Grundhoff A, Boshoff
691 C, Alitalo K, Lehti K, Ojala PM. 2011. KSHV-initiated notch activation leads to membrane-type-
692 1 matrix metalloproteinase-dependent lymphatic endothelial-to-mesenchymal transition. Cell Host
693 Microbe 10:577-90.
694 32. Lan K, Murakami M, Choudhuri T, Kuppers DA, Robertson ES. 2006. Intracellular-activated
695 Notch1 can reactivate Kaposi's sarcoma-associated herpesvirus from latency. Virology 351:393-
696 403.
697 33. Li S, Hu H, He Z, Liang D, Sun R, Lan K. 2016. Fine-Tuning of the Kaposi's Sarcoma-Associated
698 Herpesvirus Life Cycle in Neighboring Cells through the RTA-JAG1-Notch Pathway. PLOS
699 Pathogens 12:e1005900.
700 34. Curry CL, Reed LL, Golde TE, Miele L, Nickoloff BJ, Foreman KE. 2005. Gamma secretase
701 inhibitor blocks Notch activation and induces apoptosis in Kaposi's sarcoma tumor cells.
702 Oncogene 24:6333-44.
703 35. Emuss V, Lagos D, Pizzey A, Gratrix F, Henderson SR, Boshoff C. 2009. KSHV manipulates
704 Notch signaling by DLL4 and JAG1 to alter cell cycle genes in lymphatic endothelia. PLoS Pathog
705 5:e1000616.

706 36. Lan K, Murakami M, Bajaj B, Kaul R, He Z, Gan R, Feldman M, Robertson ES. 2009. Inhibition
707 of KSHV-infected primary effusion lymphomas in NOD/SCID mice by gamma-secretase
708 inhibitor. Cancer Biol Ther 8:2136-43.
709 37. Lan K, Choudhuri T, Murakami M, Kuppers DA, Robertson ES. 2006. Intracellular activated
710 Notch1 is critical for proliferation of Kaposi's sarcoma-associated herpesvirus-associated B-
711 lymphoma cell lines in vitro. J Virol 80:6411-9.
712 38. Lan K, Verma SC, Murakami M, Bajaj B, Kaul R, Robertson ES. 2007. Kaposi's sarcoma
713 herpesvirus-encoded latency-associated nuclear antigen stabilizes intracellular activated Notch by
714 targeting the Sel10 protein. Proc Natl Acad Sci U S A 104:16287-92.
715 39. Liu R, Li X, Tulpule A, Zhou Y, Scehnet JS, Zhang S, Lee JS, Chaudhary PM, Jung J, Gill PS.
716 2010. KSHV-induced notch components render endothelial and mural cell characteristics and cell
717 survival. Blood 115:887-95.
718 40. Gasperini P, Espigol-Frigole G, McCormick PJ, Salvucci O, Maric D, Uldrick TS, Polizzotto MN,
719 Yarchoan R, Tosato G. 2012. Kaposi sarcoma herpesvirus promotes endothelial-to-mesenchymal
720 transition through Notch-dependent signaling. Cancer Res 72:1157-69.
721 41. Gould F, Harrison SM, Hewitt EW, Whitehouse A. 2009. Kaposi's Sarcoma-Associated
722 Herpesvirus RTA Promotes Degradation of the Hey1 Repressor Protein through the Ubiquitin
723 Proteasome Pathway. Journal of Virology 83:6727-6738.
724 42. Green MR, Sambrook J, Sambrook J. 2012. Molecular cloning : a laboratory manual, 4th ed. Cold
725 Spring Harbor Laboratory Press, Cold Spring Harbor, N.Y.
726 43. Lukac DM, Renne R, Kirshner JR, Ganem D. 1998. Reactivation of Kaposi's Sarcoma-Associated
727 Herpesvirus Infection from Latency by Expression of the ORF 50 Transactivator, a Homolog of
728 the EBV R Protein. Virology 252:304-312.
729 44. Horn S, Kobberup S, Jørgensen MC, Kalisz M, Klein T, Kageyama R, Gegg M, Lickert H, Lindner
730 J, Magnuson MA, Kong Y-Y, Serup P, Ahnfelt-Rønne J, Jensen JN. 2012. Mind bomb
731 1 is required for pancreatic β-cell formation. Proceedings of the National Academy of
732 Sciences 109:7356-7361.
733 45. Kanda T, Sullivan KF, Wahl GM. 1998. Histone-GFP fusion protein enables sensitive analysis of
734 chromosome dynamics in living mammalian cells. Curr Biol 8:377-85.
735 46. Saxena MT, Schroeter EH, Mumm JS, Kopan R. 2001. Murine Notch Homologs (N1–4)
736 Undergo Presenilin-dependent Proteolysis *. Journal of Biological Chemistry 276:40268-40273.
737 47. Yuan Z, Friedmann DR, VanderWielen BD, Collins KJ, Kovall RA. 2012. Characterization of
738 CSL (CBF-1, Su(H), Lag-1) mutants reveals differences in signaling mediated by Notch1 and
739 Notch2. J Biol Chem 287:34904-16.
740 48. Ong CT, Cheng HT, Chang LW, Ohtsuka T, Kageyama R, Stormo GD, Kopan R. 2006. Target
741 selectivity of vertebrate notch proteins. Collaboration between discrete domains and CSL-binding
742 site architecture determines activation probability. J Biol Chem 281:5106-19.
743 49. Weng AP, Ferrando AA, Lee W, Morris JPt, Silverman LB, Sanchez-Irizarry C, Blacklow SC,
744 Look AT, Aster JC. 2004. Activating mutations of NOTCH1 in human T cell acute lymphoblastic
745 leukemia. Science 306:269-71.
746 50. Gantt S, Carlsson J, Ikoma M, Gachelet E, Gray M, Geballe AP, Corey L, Casper C, Lagunoff M,
747 Vieira J. 2011. The HIV protease inhibitor nelfinavir inhibits Kaposi's sarcoma-associated
748 herpesvirus replication in vitro. Antimicrobial agents and chemotherapy 55:2696-703.
749 51. Carroll KD, Khadim F, Spadavecchia S, Palmeri D, Lukac DM. 2007. Direct interactions of
750 Kaposi's sarcoma-associated herpesvirus/human herpesvirus 8 ORF50/Rta protein with the
751 cellular protein octamer-1 and DNA are critical for specifying transactivation of a delayed-early
752 promoter and stimulating viral reactivation. J Virol 81:8451-67.

753 52. Kirshner JR, Lukac DM, Chang J, Ganem D. 2000. Kaposi's Sarcoma-Associated Herpesvirus
754 Open Reading Frame 57 Encodes a Posttranscriptional Regulator with Multiple Distinct Activities.
755 J Virol 74:3586-3597.
756 53. Bruce AG, Barcy S, DiMaio T, Gan E, Garrigues HJ, Lagunoff M, Rose TM. 2017. Quantitative
757 Analysis of the KSHV Transcriptome Following Primary Infection of Blood and Lymphatic
758 Endothelial Cells. Pathogens 6.
759 54. Journo G, Tushinsky C, Shterngas A, Avital N, Eran Y, Karpuj MV, Frenkel-Morgenstern M,
760 Shamay M. 2018. Modulation of Cellular CpG DNA Methylation by Kaposi's Sarcoma-Associated
761 Herpesvirus. J Virol 92.
762 55. Gonzalez-Lopez O, Goyeneche, C, DeCotiis, J Vicente-Ortiz, BA, Shin H, Driscoll, K, Du P,
763 Palmeri, D, and DM Lukac. 2019. Viral Rta and cellular POU proteins regulate dynamic, genome-
764 wide DNA binding of the Notch pathway protein Recombination Signal Binding Protein (RBP)-
765 Jk during reactivation of Kaposi's sarcoma-associated herpesvirus (KSHV). Submitted.
766 56. Nelson JD, Denisenko O, Bomsztyk K. 2006. Protocol for the fast chromatin immunoprecipitation
767 (ChIP) method. Nature Protocols 1:179-185.
768 57. Güner G, Lichtenthaler SF. 2020. The substrate repertoire of γ-secretase/presenilin. Seminars in
769 Cell & Developmental Biology 105:27-42.
770 58. Weng AP, Nam Y, Wolfe MS, Pear WS, Griffin JD, Blacklow SC, Aster JC. 2003. Growth
771 Suppression of Pre-T Acute Lymphoblastic Leukemia Cells by Inhibition of Notch Signaling.
772 Molecular and Cellular Biology 23:655-664.
773 59. Zema S, Pelullo M, Nardozza F, Felli MP, Screpanti I, Bellavia D. 2020. A Dynamic Role of
774 Mastermind-Like 1: A Journey Through the Main (Path)ways Between Development and Cancer.
775 Frontiers in Cell and Developmental Biology 8.
776 60. Maillard I, Weng AP, Carpenter AC, Rodriguez CG, Sai H, Xu L, Allman D, Aster JC, Pear WS.
777 2004. Mastermind critically regulates Notch-mediated lymphoid cell fate decisions. Blood
778 104:1696-1702.
779 61. Saravanamuthu SS, Gao CY, Zelenka PS. 2009. Notch signaling is required for lateral induction
780 of Jagged1 during FGF-induced lens fiber differentiation. Dev Biol 332:166-76.
781 62. Bagheri L, Pellati A, Rizzo P, Aquila G, Massari L, De Mattei M, Ongaro A. 2018. Notch pathway
782 is active during osteogenic differentiation of human bone marrow mesenchymal stem cells induced
783 by pulsed electromagnetic fields. J Tissue Eng Regen Med 12:304-315.
784 63. Lilly B, Kennard S. 2009. Differential gene expression in a coculture model of angiogenesis
785 reveals modulation of select pathways and a role for Notch signaling. Physiol Genomics 36:69-78.
786 64. Sastre M, Steiner H, Fuchs K, Capell A, Multhaup G, Condron MM, Teplow DB, Haass C. 2001.
787 Presenilin-dependent γ-secretase processing of β-amyloid precursor protein at a site corresponding
788 to the S3 cleavage of Notch. EMBO reports 2:835-841.
789 65. Shin HJ, Decotiis J, Giron M, Palmeri D, Lukac DM. 2014. Histone Deacetylase Classes I and II
790 Regulate Kaposi's Sarcoma-Associated Herpesvirus Reactivation. J Virol 88:1281-92.
791 66. Chiang MY, Xu L, Shestova O, Histen G, L'Heureux S, Romany C, Childs ME, Gimotty PA, Aster
792 JC, Pear WS. 2008. Leukemia-associated NOTCH1 alleles are weak tumor initiators but accelerate
793 K-ras-initiated leukemia. J Clin Invest 118:3181-94.
794 67. Beatus P, Lundkvist J, Oberg C, Pedersen K, Lendahl U. 2001. The origin of the ankyrin repeat
795 region in Notch intracellular domains is critical for regulation of HES promoter activity. Mech
796 Dev 104:3-20.
797 68. James AC, Szot JO, Iyer K, Major JA, Pursglove SE, Chapman G, Dunwoodie SL. 2014. Notch4
798 reveals a novel mechanism regulating Notch signal transduction. Biochim Biophys Acta
799 1843:1272-84.

800 69. Yamaguchi N, Oyama T, Ito E, Satoh H, Azuma S, Hayashi M, Shimizu K, Honma R, Yanagisawa
801 Y, Nishikawa A, Kawamura M, Imai J-i, Ohwada S, Tatsuta K, Inoue J-i, Semba K, Watanabe S.
802 2008. NOTCH3 Signaling Pathway Plays Crucial Roles in the Proliferation of ErbB2-Negative
803 Human Breast Cancer Cells. Cancer Research 68:1881-1888.
804 70. Liu Z, Brunskill E, Varnum-Finney B, Zhang C, Zhang A, Jay PY, Bernstein I, Morimoto M,
805 Kopan R. 2015. The intracellular domains of Notch1 and Notch2 are functionally equivalent
806 during development and carcinogenesis. Development 142:2452-2463.
807 71. Giachino C, Boulay JL, Ivanek R, Alvarado A, Tostado C, Lugert S, Tchorz J, Coban M, Mariani
808 L, Bettler B, Lathia J, Frank S, Pfister S, Kool M, Taylor V. 2015. A Tumor Suppressor Function
809 for Notch Signaling in Forebrain Tumor Subtypes. Cancer Cell 28:730-742.
810 72. Rossi D, Trifonov V, Fangazio M, Bruscaggin A, Rasi S, Spina V, Monti S, Vaisitti T, Arruga F,
811 Famà R, Ciardullo C, Greco M, Cresta S, Piranda D, Holmes A, Fabbri G, Messina M, Rinaldi A,
812 Wang J, Agostinelli C, Piccaluga PP, Lucioni M, Tabbò F, Serra R, Franceschetti S, Deambrogi
813 C, Daniele G, Gattei V, Marasca R, Facchetti F, Arcaini L, Inghirami G, Bertoni F, Pileri SA,
814 Deaglio S, Foà R, Dalla-Favera R, Pasqualucci L, Rabadan R, Gaidano G. 2012. The coding
815 genome of splenic marginal zone lymphoma: activation of NOTCH2 and other pathways
816 regulating marginal zone development. Journal of Experimental Medicine 209:1537-1551.
817 73. De Strooper B, Annaert W, Cupers P, Saftig P, Craessaerts K, Mumm JS, Schroeter EH, Schrijvers
818 V, Wolfe MS, Ray WJ, Goate A, Kopan R. 1999. A presenilin-1-dependent γ-secretase-like
819 protease mediates release of Notch intracellular domain. Nature 398:518-522.
820 74. Lin SE, Oyama T, Nagase T, Harigaya K, Kitagawa M. 2002. Identification of new human
821 mastermind proteins defines a family that consists of positive regulators for notch signaling. J Biol
822 Chem 277:50612-20.
823 75. Wu L, Sun T, Kobayashi K, Gao P, Griffin JD. 2002. Identification of a family of mastermind-like
824 transcriptional coactivators for mammalian notch receptors. Mol Cell Biol 22:7688-700.
825 76. DiMaio D. 2019. Small size, big impact: how studies of small DNA tumour viruses revolutionized
826 biology. Philos Trans R Soc Lond B Biol Sci 374:20180300.
827 77. Siebel C, Lendahl U. 2017. Notch Signaling in Development, Tissue Homeostasis, and Disease.
828 Physiol Rev 97:1235-1294.
829 78. Sprinzak D, Blacklow SC. 2021. Biophysics of Notch Signaling. Annu Rev Biophys 50:157-189.
830 79. Wang H, Zang C, Taing L, Arnett KL, Wong YJ, Pear WS, Blacklow SC, Liu XS, Aster JC. 2014.
831 NOTCH1-RBPJ complexes drive target gene expression through dynamic interactions with
832 superenhancers. Proc Natl Acad Sci U S A 111:705-10.
833 80. Castel D, Mourikis P, Bartels SJ, Brinkman AB, Tajbakhsh S, Stunnenberg HG. 2013. Dynamic
834 binding of RBPJ is determined by Notch signaling status. Genes Dev 27:1059-71.
835 81. Krejci A, Bray S. 2007. Notch activation stimulates transient and selective binding of Su(H)/CSL
836 to target enhancers. Genes Dev 21:1322-7.
837 82. Gomez-Lamarca MJ, Falo-Sanjuan J, Stojnic R, Abdul Rehman S, Muresan L, Jones ML, Pillidge
838 Z, Cerda-Moya G, Yuan Z, Baloul S, Valenti P, Bystricky K, Payre F, O'Holleran K, Kovall R,
839 Bray SJ. 2018. Activation of the Notch Signaling Pathway In Vivo Elicits Changes in CSL Nuclear
840 Dynamics. Developmental Cell 44:611-623.e7.
841 83. Zhao B, Zou J, Wang H, Johannsen E, Peng CW, Quackenbush J, Mar JC, Morton CC, Freedman
842 ML, Blacklow SC, Aster JC, Bernstein BE, Kieff E. 2011. Epstein-Barr virus exploits intrinsic B-
843 lymphocyte transcription programs to achieve immortal cell growth. Proc Natl Acad Sci U S A
844 108:14902-7.
845 84. Severson E, Arnett KL, Wang H, Zang C, Taing L, Liu H, Pear WS, Shirley Liu X, Blacklow SC,
846 Aster JC. 2017. Genome-wide identification and characterization of Notch transcription complex–
847 binding sequence-paired sites in leukemia cells. Science Signaling 10:eaag1598.

848 85. Ryan RJH, Petrovic J, Rausch DM, Zhou Y, Lareau CA, Kluk MJ, Christie AL, Lee WY, Tarjan
849 DR, Guo B, Donohue LKH, Gillespie SM, Nardi V, Hochberg EP, Blacklow SC, Weinstock DM,
850 Faryabi RB, Bernstein BE, Aster JC, Pear WS. 2017. A B Cell Regulome Links Notch to
851 Downstream Oncogenic Pathways in Small B Cell Lymphomas. Cell Reports 21:784-797.
852 86. Yashiro-Ohtani Y, Wang H, Zang C, Arnett KL, Bailis W, Ho Y, Knoechel B, Lanauze C, Louis
853 L, Forsyth KS, Chen S, Chung Y, Schug J, Blobel GA, Liebhaber SA, Bernstein BE, Blacklow
854 SC, Liu XS, Aster JC, Pear WS. 2014. Long-range enhancer activity determines Myc
855 sensitivity to Notch inhibitors in T cell leukemia. Proceedings of the National Academy of
856 Sciences doi:10.1073/pnas.1407079111:201407079.
857 87. Song M, Brown H, Wu T-T, Sun R. 2001. Transcription activation of polyadenylated nuclear RNA
858 by Rta in Human herpesvirus 8/Kaposi's Sarcoma-associated herpesvirus. J Virol 75:3129-40.
859 88. Chen J, Ye F, Xie J, Kuhne K, Gao SJ. 2009. Genome-wide identification of binding sites for
860 Kaposi's sarcoma-associated herpesvirus lytic switch protein, RTA. Virology 386:290-302.
861 89. Wang Y, Li H, Chan MY, Zhu FX, Lukac DM, Yuan Y. 2004. Kaposi's sarcoma-associated
862 herpesvirus ori-Lyt-dependent DNA replication: cis-acting requirements for replication and ori-
863 Lyt-associated RNA transcription. J Virol 78:8615-29.
864 90. Rossetto CC, Susilarini NK, Pari GS. 2011. Interaction of Kaposi's sarcoma-associated herpesvirus
865 ORF59 with oriLyt is dependent on binding with K-Rta. J Virol 85:3833-41.
866 91. Castro B, Barolo S, Bailey AM, Posakony JW. 2005. Lateral inhibition in proneural clusters: cis-
867 regulatory logic and default repression by Suppressor of Hairless. Development 132:3333-3344.
868 92. Nellesen DT, Lai EC, Posakony JW. 1999. Discrete enhancer elements mediate selective
869 responsiveness of enhancer of split complex genes to common transcriptional activators. Dev Biol
870 213:33-53.
871 93. Wang H, Zou J, Zhao B, Johannsen E, Ashworth T, Wong H, Pear WS, Schug J, Blacklow SC,
872 Arnett KL, Bernstein BE, Kieff E, Aster JC. 2011. Genome-wide analysis reveals conserved and
873 divergent features of Notch1/RBPJ binding in human and murine T-lymphoblastic leukemia cells.
874 Proc Natl Acad Sci U S A 108:14908-13.
875 94. Swanson CI, Evans NC, Barolo S. 2010. Structural rules and complex regulatory circuitry
876 constrain expression of a Notch- and EGFR-regulated eye enhancer. Dev Cell 18:359-70.
877 95. Cooper MT, Tyler DM, Furriols M, Chalkiadaki A, Delidakis C, Bray S. 2000. Spatially restricted
878 factors cooperate with notch in the regulation of Enhancer of split genes. Dev Biol 221:390-403.
879 96. Cave JW, Loh F, Surpris JW, Xia L, Caudy MA. 2005. A DNA transcription code for cell-specific
880 gene activation by notch signaling. Curr Biol 15:94-104.
881 97. Takebayashi K, Sasai Y, Sakai Y, Watanabe T, Nakanishi S, Kageyama R. 1994. Structure,
882 chromosomal locus, and promoter analysis of the gene encoding the mouse helix-loop-helix factor
883 HES-1. Negative autoregulation through the multiple N box elements. J Biol Chem 269:5150-6.
884 98. Basak O, Giachino C, Fiorini E, MacDonald HR, Taylor V. 2012. Neurogenic Subventricular Zone
885 Stem/Progenitor Cells Are Notch1-Dependent in Their Active But Not Quiescent State. The
886 Journal of Neuroscience 32:5654-5666.
887 99. Stoeck A, Lejnine S, Truong A, Pan L, Wang H, Zang C, Yuan J, Ware C, MacLean J, Garrett-
888 Engele PW, Kluk M, Laskey J, Haines BB, Moskaluk C, Zawel L, Fawell S, Gilliland G, Zhang
889 T, Kremer BE, Knoechel B, Bernstein BE, Pear WS, Liu XS, Aster JC, Sathyanarayanan S. 2014.
890 Discovery of biomarkers predictive of GSI response in triple-negative breast cancer and adenoid
891 cystic carcinoma. Cancer Discov 4:1154-67.
892 100. Krejcí A, Bernard F, Housden BE, Collins S, Bray SJ. 2009. Direct response to Notch activation:
893 signaling crosstalk and incoherent logic. Sci Signal 2:ra1.

894 101. Choi SH, Severson E, Pear WS, Liu XS, Aster JC, Blacklow SC. 2017. The common oncogenomic
895 program of NOTCH1 and NOTCH3 signaling in T-cell acute lymphoblastic leukemia. PLOS ONE
896 12:e0185762.
897 102. Bellavia D, Campese AF, Checquolo S, Balestri A, Biondi A, Cazzaniga G, Lendahl U, Fehling
898 HJ, Hayday AC, Frati L, von Boehmer H, Gulino A, Screpanti I. 2002. Combined expression of
899 pTα and Notch3 in T cell leukemia identifies the requirement of preTCR for leukemogenesis.
900 Proceedings of the National Academy of Sciences 99:3788-3793.
901 103. Engler A, Rolando C, Giachino C, Saotome I, Erni A, Brien C, Zhang R, Zimber-Strobl U, Radtke
902 F, Artavanis-Tsakonas S, Louvi A, Taylor V. 2018. Notch2 Signaling Maintains NSC Quiescence
903 in the Murine Ventricular-Subventricular Zone. Cell Reports 22:992-1002.
904 104. Meester JAN, Verstraeten A, Alaerts M, Schepers D, Van Laer L, Loeys BL. 2019. Overlapping
905 but distinct roles for NOTCH receptors in human cardiovascular disease. Clinical Genetics 95:85-
906 94.
907 105. Beatus P, Lundkvist J, Oberg C, Lendahl U. 1999. The notch 3 intracellular domain represses
908 notch 1-mediated activation through Hairy/Enhancer of split (HES) promoters. Development
909 126:3925-3935.
910 106. Beà S, Valdés-Mas R, Navarro A, Salaverria I, Martín-Garcia D, Jares P, Giné E, Pinyol M, Royo
911 C, Nadeu F, Conde L, Juan M, Clot G, Vizán P, Di Croce L, Puente DA, López-Guerra M, Moros
912 A, Roue G, Aymerich M, Villamor N, Colomo L, Martínez A, Valera A, Martín-Subero JI,
913 Amador V, Hernández L, Rozman M, Enjuanes A, Forcada P, Muntañola A, Hartmann EM,
914 Calasanz MJ, Rosenwald A, Ott G, Hernández-Rivas JM, Klapper W, Siebert R, Wiestner A,
915 Wilson WH, Colomer D, López-Guillermo A, López-Otín C, Puente XS, Campo E. 2013.
916 Landscape of somatic mutations and clonal evolution in mantle cell lymphoma. Proceedings of the
917 National Academy of Sciences 110:18250-18255.
918 107. Ables JL, DeCarolis NA, Johnson MA, Rivera PD, Gao Z, Cooper DC, Radtke F, Hsieh J, Eisch
919 AJ. 2010. Notch1 Is Required for Maintenance of the Reservoir of Adult Hippocampal Stem Cells.
920 The Journal of Neuroscience 30:10484-10492.
921 108. Nwabo Kamdje AH, Bassi G, Pacelli L, Malpeli G, Amati E, Nichele I, Pizzolo G, Krampera M.
922 2012. Role of stromal cell-mediated Notch signaling in CLL resistance to chemotherapy. Blood
923 Cancer Journal 2:e73-e73.
924 109. Demehri S, Turkoz A, Manivasagam S, Yockey Laura J, Turkoz M, Kopan R. 2012. Elevated
925 Epidermal Thymic Stromal Lymphopoietin Levels Establish an Antitumor Environment in the
926 Skin. Cancer Cell 22:494-505.
927 110. Boucher JM, Harrington A, Rostama B, Lindner V, Liaw L. 2013. A Receptor-Specific Function
928 for Notch2 in Mediating Vascular Smooth Muscle Cell Growth Arrest Through Cyclin-dependent
929 Kinase Inhibitor 1B. Circulation Research 113:975-985.
930 111. Southgate L, Sukalo M, Karountzos ASV, Taylor EJ, Collinson CS, Ruddy D, Snape KM,
931 Dallapiccola B, Tolmie JL, Joss S, Brancati F, Digilio MC, Graul-Neumann LM, Salviati L, Coerdt
932 W, Jacquemin E, Wuyts W, Zenker M, Machado RD, Trembath RC. 2015. Haploinsufficiency of
933 the NOTCH1 Receptor as a Cause of Adams–Oliver Syndrome With Variable Cardiac
934 Anomalies. Circulation: Cardiovascular Genetics 8:572-581.
935 112. Kawai H, Kawaguchi D, Kuebrich BD, Kitamoto T, Yamaguchi M, Gotoh Y, Furutachi S. 2017.
936 Area-Specific Regulation of Quiescent Neural Stem Cells by Notch3 in the Adult Mouse
937 Subependymal Zone. The Journal of Neuroscience 37:11867-11880.
938 113. Arasada RR, Amann JM, Rahman MA, Huppert SS, Carbone DP. 2014. EGFR blockade enriches
939 for lung cancer stem-like cells through Notch3-dependent signaling. Cancer Research
940 doi:10.1158/0008-5472.Can-13-3724:canres.3724.2013.

941 114. Kofler NM, Cuervo H, Uh MK, Murtomäki A, Kitajewski J. 2015. Combined deficiency of Notch1
942 and Notch3 causes pericyte dysfunction, models CADASIL and results in arteriovenous
943 malformations. Scientific Reports 5:16449.
944 115. Arruga F, Vaisitti T, Deaglio S. 2018. The NOTCH Pathway and Its Mutations in Mature B Cell
945 Malignancies. Frontiers in Oncology 8.
946 116. Parmigiani E, Taylor V, Giachino C. 2020. Oncogenic and Tumor-Suppressive Functions of
947 NOTCH Signaling in Glioma. Cells 9:2304.
948 117. D'Assoro AB, Leon-Ferre R, Braune EB, Lendahl U. 2022. Roles of Notch Signaling in the Tumor
949 Microenvironment. Int J Mol Sci 23.
950 118. Nam Y, Sliz P, Pear WS, Aster JC, Blacklow SC. 2007. Cooperative assembly of higher-order
951 Notch complexes functions as a switch to induce transcription. Proc Natl Acad Sci U S A
952 104:2103-8.
953 119. Nam Y, Sliz P, Song L, Aster JC, Blacklow SC. 2006. Structural basis for cooperativity in
954 recruitment of MAML coactivators to Notch transcription complexes. Cell 124:973-83.
955 120. Arnett KL, Hass M, McArthur DG, Ilagan MX, Aster JC, Kopan R, Blacklow SC. 2010. Structural
956 and mechanistic insights into cooperative assembly of dimeric Notch transcription complexes. Nat
957 Struct Mol Biol 17:1312-7.
958 121. Liu H, Chi AW, Arnett KL, Chiang MY, Xu L, Shestova O, Wang H, Li YM, Bhandoola A, Aster
959 JC, Blacklow SC, Pear WS. 2010. Notch dimerization is required for leukemogenesis and T-cell
960 development. Genes Dev 24:2395-407.

961

962

963 **FIGURE LEGENDS**

964 **Figure 1. Endogenous Notch1 is constitutively active in infected Vero cells.** Total cellular protein
965 was harvested in RIPA buffer from triplicate cultures of 4 x 10^5 cells Vero rKSHV.294 cells at time of
966 plating ("0h") or 24h after plating. 20 ugs from each extract were separated on a 4-12% PAGE gradient
967 gel electrophoresed in Tris-MOPS-SDS buffer. The NICD1 control lane ("Con") contains equal total
968 protein from uninfected Vero cells transfected with NICD1 expression vector pCMV-NICD1. Proteins
969 transferred to nitrocellulose were probed with Notch1-specific bTAN20 antibody (1:500) or anti-GAPDH
970 antibody (1:5000), followed by HRP-conjugated anti-Rat secondary antibody (1:5000). Bands were
971 visualized by ChemiDoc (BioRad).

972
973
974 **Figure 2. Notch inhibition reduces Rta-mediated reactivation without inhibiting cell growth.**
975

976 **A. Treatment with a gamma secretase inhibitor decreases viral reactivation by Rta.** Vero
977 rKSHV.294 cells were treated with 1 or 5 uM DAPT, or vehicle control ("Vh") 24h prior to transfection
978 with 2.5 ug of Rta expression vector. At 72h post-transfection, infectious virus was quantitated by
979 transferring the media to the 293 MSR tet-OFF complementing reporter cells as described in Methods.
980 SeAP was measured in 25 uL of media per infection using the Phospha-Light System (Applied
981 Biosystems). SeAP values from media alone were subtracted from each experimental value, and folds
982 were calculated by normalizing to samples treated with vehicle and transfected with empty vector.
983 *$p<0.05$ by t test compared to Vec + Vh.

984 **B. Treatment with a gamma secretase inhibitor decreases activity of a Notch-dependent reporter**
985 **plasmid.** Vero rKSHV.294 cells were transfected with Notch reporter plasmid pGL2-4xCSL expressing
986 firefly luciferase ("Jk") and pcDNA3.1-HisLacZ expressing β-galactosidase ("Cont"). Cells were treated
987 with 5 uM DAPT or vehicle (DMSO) 24hr post-transfection, and total cellular protein was extracted.
988 Luciferase values were normalized to βgal values at each timepoint. *$p<0.0015$ and **$p<0.0001$ by t test
989 compared to Cont at each time point.

990 **C. Notch inhibition by DAPT treatment does not affect Vero rKSHV.294 cell growth.** Triplicate
991 cultures of Vero rKSHV.294 cells were treated with vehicle or DAPT at the indicated concentrations as
992 described in Fig 2A. At the post-treatment times indicated, cell viability was quantitated using Alamar
993 Blue (BioRad). Mock values were averaged and subtracted from each experimental value to yield
994 corrected values. All corrected values were then normalized to 0h values that had been set to the
995 relative value of 1 for each treatment. The slight enhancement of cell growth rate when compared to the
996 vehicle control was not statistically-significant.

997 **D. and E. Expression of KSHV transcripts are reduced by inhibiting endogenous Notch1.**
998 Triplicate cultures of Vero rKSHV.294 cells were transfected with empty vector or Rta expression
999 vector and treated with vehicle or DAPT (5 uM DAPT), as in Fig 2A. Total RNA was harvested 24 h

1000 after transfection and transcripts for the indicated viral genes were quantitated by real-time quantitative
1001 reverse-transcription/PCR. Transcription of the indicated viral genes was calculated by the delta-delta Ct
1002 method using cellular beta-actin transcription as the internal control for each sample and Vec + vehicle
1003 as baseline fold. One outlying value per transfection was removed using Peirce's method. *p<0.05 by t
1004 test comparing Rta + vehicle (DMSO) to Rta + 5 uM DAPT**.** Each primer pair was also tested without
1005 adding reverse transcriptase to the input RNA and no amplicons were detected (not shown).

1006

1007 **Fig 3. Inhibition of endogenous Notch by dominant negative MAML1 mutants inhibit viral**
1008 **reactivation and expression of some viral genes. A.** Vero rKSHV.294 cells were transfected with 1ug
1009 of plasmids expressing Rta and two different dnMAML alleles ("dnMAM" "A" and "B"; each fused to
1010 GFP). Infectious virus was quantitated as in Fig. 2A. *p<0.02 and **p<0.01 by t test compared to Rta
1011 plus Vector. **B. dnMAML1 proteins are well-expressed in infected Vero rKSHV.294 cells.** Vero
1012 rKSHV.294 cells were transfected as in Fig 3A, total protein was harvested in RIPA buffer 48h later,
1013 Western blotted, and probed with GFP-specific antiserum to detect the dnMAML-GFP fusion proteins.
1014 As a control for the Western blot, plasmid expressing H2b-GFP was also transfected into cells ("H2b").
1015 **C. Expression of KSHV proteins are reduced by inhibiting endogenous Notch1.** Expression of the
1016 KSHV proteins Mta, KbZIP, and ORF59 in extracts from cells transfected as in Fig 3B were visualized
1017 by Western blotting. Fold induction of each viral protein was determined by normalizing to expression
1018 of the host protein Histone H3 ("H3") in each lane, then dividing by the value for Vec alone, which had
1019 been set to "1." Those values are listed under each corresponding lane. **D.** Quantitation. The relative
1020 reduction of viral protein expression by inhibiting Notch1 was calculated by comparing each viral
1021 protein's induction by ectopic Rta + Vec with that induced by Rta in the presence of ectopic dnMAML1
1022 in panel B. Rta alone was set at 100. *p<0.09 and **p<0.005 by t test compared to Rta + Vec**.**
1023

1024 **Fig 4. Activated Notch1 is required for optimal reactivation of KSHV. A. Reactivation by ectopic**
1025 **Rta.** Vero rKSHV.294 cells were transfected with 30 pM of either scrambled siRNA (Scr; control),
1026 Notch 1 siRNA A (N1-A), or Notch 1 siRNA B (N1-B) in triplicate sets. 48h later, Rta expression
1027 vector or Vec (as control) was transfected into each of the siRNA-transfected cells. 48h post-
1028 transfection, virus containing media were transferred to 293 MSR tet-OFF cells. Infectious virus was
1029 quantitated as in Fig. 2A. *p<0.02 by t test compared to Rta + Scr **. B. Reactivation by VPA treatment.**
1030 Vero rKSHV.294 cells were transfected with 30pM of either scrambled siRNA (Scr; control) or Notch 1
1031 siRNA B (N1-B). 54h later, 1 mM VPA was added to the siRNA-transfected cells. 72h post-
1032 transfection, virus containing media were transferred to 293 MSR tet-OFF cells. Infectious virus was
1033 quantitated as in Fig. 2A. **C. siRNA specifically reduces NICD1 expression.** Vero rKSHV.294 cells
1034 were transfected with 30pM of the siRNAs described in the legend to Fig. 4A. 48h post transfection,
1035 total cellular proteins were extracted in RIPA buffer, then analyzed via a 10% SDS-PAGE/western blot
1036 as described in the legend to Fig. 1A.
1037
1038
1039 **Fig. 5. Activated Notch binds to KSHV promoters during reactivation.** Triplicate cultures of Vero
1040 rKSHV.294 cells were transfected with empty vector or Rta expression vector in three experiments.
1041 Cross-linked chromatin was sonicated and immunoprecipitated (ChIP'd) with NICD1-specific antibody
1042 or non-specific IgG control. ChIP'd DNA was purified and analyzed by quantitative real-time PCR to
1043 detect sequences located within 1 kb. upstream of the transcriptional start sites of the indicated KSHV
1044 genes. Fold increases in ChIP'd promoters were calculated by the delta-delta Ct method using non-
1045 specific IgG as the internal control for each sample and EV transfection as baseline fold. Folds were
1046 normalized by comparison to NICD1 expression in transfected samples. *=All amplicons were
1047 significantly increased (t test p value <0.05) in Rta samples compared to EV.
1048

1049

1050 **Fig. 6. Activated Notch1 is required for optimal reactivation of KSHV in infected PEL cells. A.**
1051 **DAPT inhibits vDNA accumulation in PEL cells.** Triplicate cultures of KSHV-infected BC3 cells were
1052 treated with vehicle alone ("Vh") or containing 16, 32, or 40 uM DAPT for 65h. Total DNA was purified
1053 using the FlexiGene DNA kit (Qiagen). Intracellular viral DNA was measured by real-time quantitative
1054 (q) PCR using SYBR Green PCR Master Mix (Thermo Scientific) and GAPDH was the internal control.
1055 Fold-DNA was calculated using the ΔCt method and all values were normalized to that of VPA + vehicle
1056 alone, which was set to 100%. *$p<0.03$, **$p<0.009$, and ***$p<0.006$ by t test compared to VPA+Veh.
1057 **B. Gene-specific expression of KSHV genes is reduced by Notch inhibition in PEL cells.** Triplicate
1058 cultures of KSHV-infected BCBL1 cells were treated with 1 mM VPA and vehicle ("Vh") or DAPT (16,
1059 32, or 40 uM). 48 or 72h post-treatment, ORF59 and K8.1 were detected by indirect immunofluorescence,
1060 respectively. The percentages of ORF59 or K8.1 positive cells were quantitated, and fold-percent positive
1061 cells were calculated by normalizing to samples treated with vehicle alone. *$p<0.007$ and **$p<0.005$ by
1062 t test compared to VPA+Veh.

1063
1064
1065 **Fig. 7. Ectopic NICD 1-4 are not sufficient to induce KSHV reactivation. A.** Vero rKSHV.294 cells
1066 were transfected with 2.5 ug plasmid DNA expressing each of the indicated proteins and incubated for
1067 72h at which time virus containing media were transferred to 293 MSR tet-OFF cells. Infectious virus
1068 was quantitated as in the legend to Fig. 2A, using the Great EscAPe SeAP kit (Takara). T test was used
1069 to determine that only samples transfected with Rta induced significant viral reactivation ($p<0.05$
1070 compared to Vec). **B. All four constitutively active Notch isoforms are expressed ectopically in**
1071 **transfected Vero rKSHV.294 cells.** Cells were transfected as in the legend to Fig 7A, and total proteins
1072 were harvested in RIPA buffer 48h later, Western blotted, and probed with FLAG-tag and tubulin-specific
1073 antibodies. All Notch isoforms were observed at the appropriate apparent MWs (48).

1074

1075 **Figure 8. Ectopic Notch isoforms 1 and 2 are transactivation competent in Vero rKSHV.294 cells.**

1076 Triplicate cultures of Vero rKSHV.294 cells were transfected with 0.25 ug of the Notch reporter plasmid

1077 4xCBS expressing firefly luciferase, control plasmid pcDNA3.1-HisLacZ expressing β-galactosidase

1078 (βgal) and 3 ug of each of the four Notch isoform vectors. Extracts were made 48 h post-transfection, and

1079 raw luciferase values were corrected to β-galactosidase. Folds were calculated by normalization to

1080 samples transfected with luciferase reporter and empty vector (Vec) alone. *$p<0.02$ and **$p<0.0001$ by t

1081 test compared to Vec.

1082

1083

1084 **Figure 9. Ectopic NICD1 alleles with varying intrinsic activities are not sufficient to induce KSHV**

1085 **reactivation.** Vero rKSHV.294 cells were transfected with 2.5 ug plasmid DNA expressing each of the

1086 indicated proteins and incubated for 72h at which time virus containing media were transferred to 293

1087 MSR tet-OFF cells. Infectious virus was quantitated as in Fig. 2A, using the Great EscAPe SeAP kit

1088 (Takara).

1089

1090 **Fig. 10. Ectopic NICD1 cooperates with VPA in KSHV reactivation.** Vero rKSHV.294 cells were

1091 transfected with 1 ug plasmid DNA expressing NICD1 ("N1") or empty vector. 18 h post-transfection,

1092 cells were treated with 1 mM VPA. 72 h post-treatment, virus containing media were transferred to 293

1093 MSR tet-OFF cells. Infectious virus was quantitated as in Fig 2A.

DeCotiis-Mauro, Han, et al, Fig 1

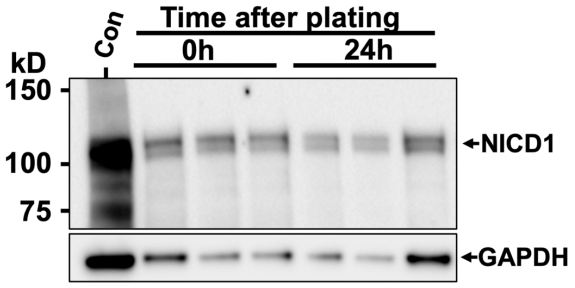

DeCotiis-Mauro, Han, et al Fig 2

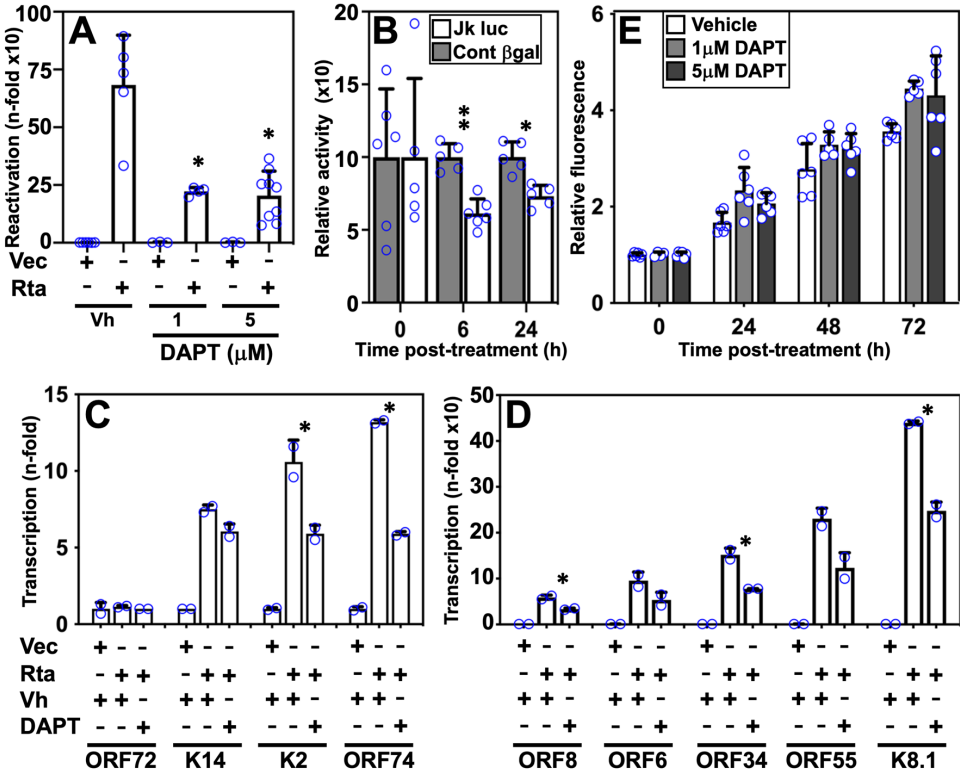

DeCotiis-Mauro, Han, et al Fig 3

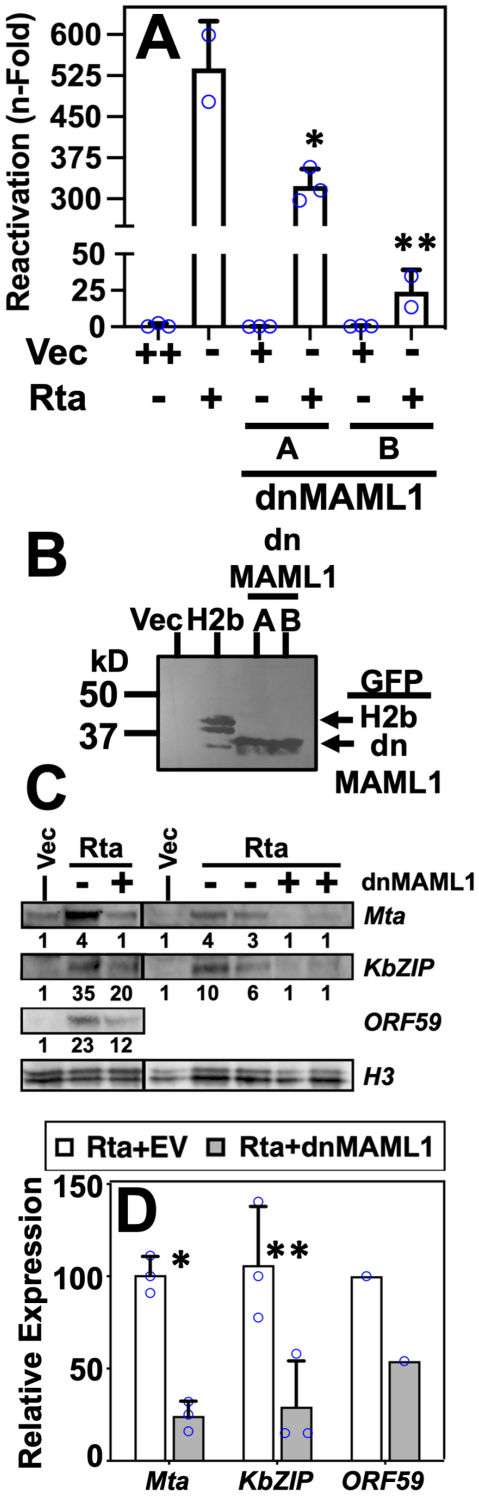

DeCotiis-Mauro, Han, et al Fig 4

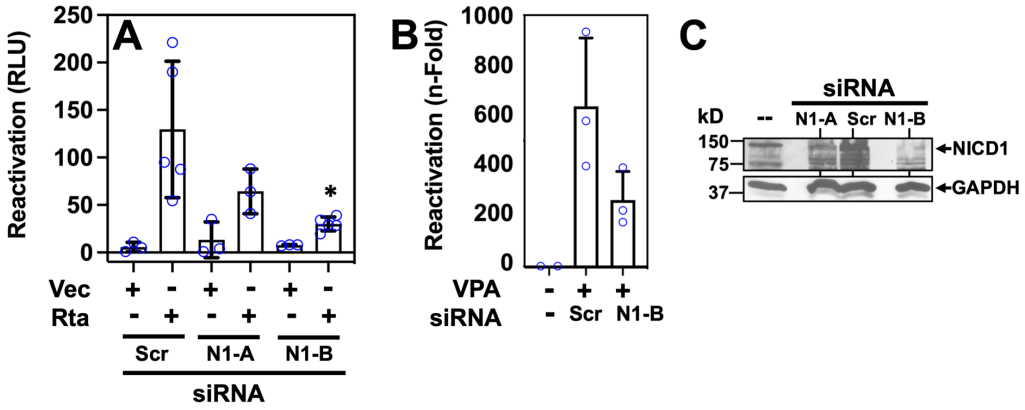

DeCotiis-Mauro, Han, et al Fig 5

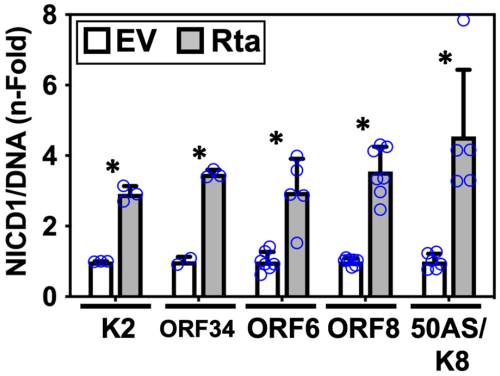

DeCotiis-Mauro, Han, et al Fig 6

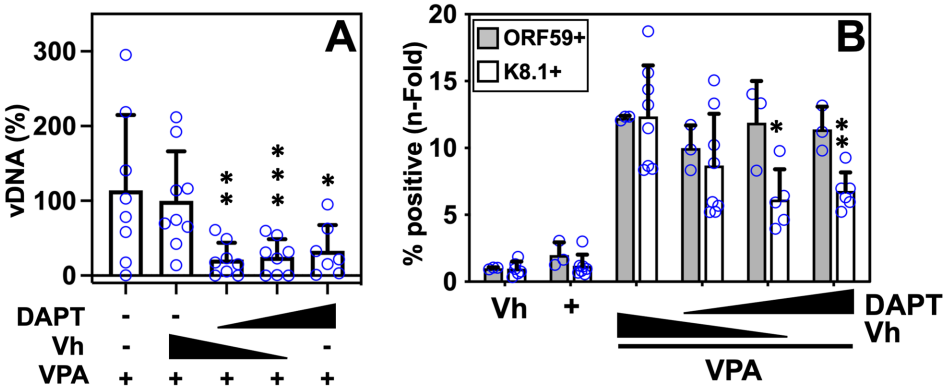

DeCotiis-Mauro, Han, et al Fig 7

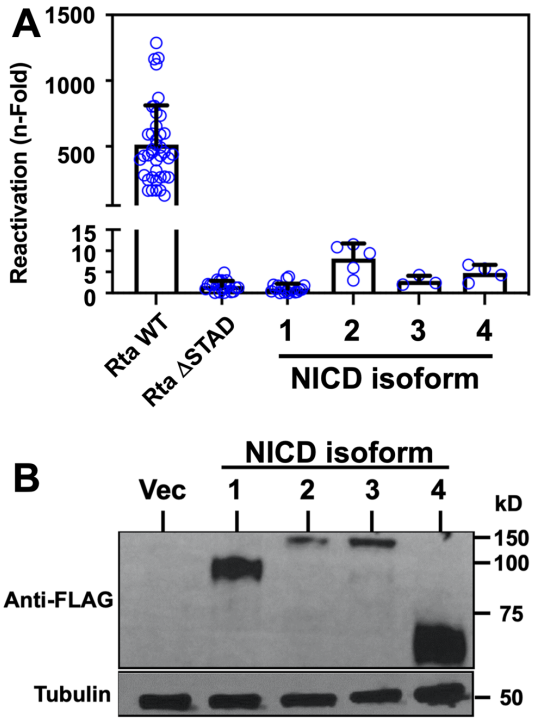

DeCotiis-Mauro, Han, et al Fig 8

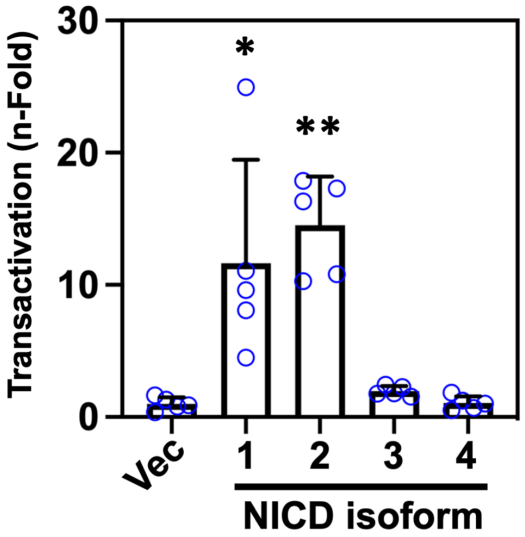

DeCotiis-Mauro, Han, et al. Fig 9

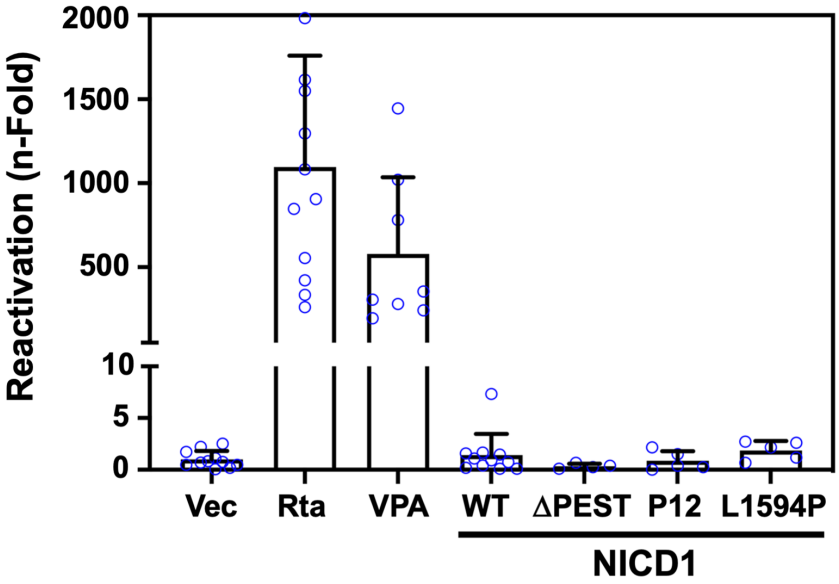
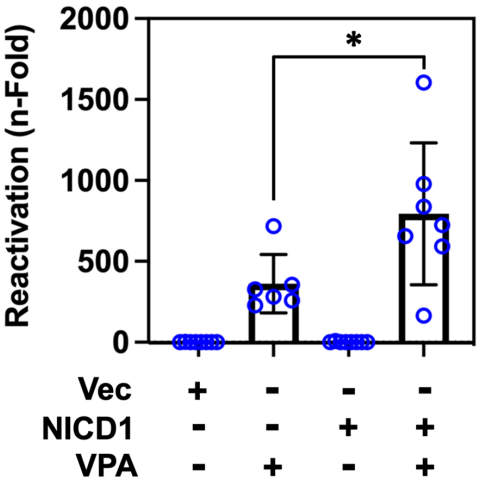
DeCotiis-Mauro, Han, et al Fig 10